Biogeosciences Discuss., https://doi.org/10.5194/bg-2017-537
Manuscript under review for journal Biogeosciences
Discussion started: 3 January 2018

Biogeosciences Discussions
Open Access
EGU

Deep-sea benthic communities and oxygen fluxes in the Arctic Fram Strait controlled by sea-ice cover and water depth

Ralf Hoffmann[1], Ulrike Braeckman[2,3], Christiane Hasemann[1], Frank Wenzhöfer[1, 3]

[1]Alfred Wegener Institute, Helmholtz Centre for Polar- and Marine Research, Am Handelshafen 12, 27570 Bremerhaven, Germany
[2]Ghent University, Marine Biology Research Group, Krijgslaan 281 S8, 9000 Gent, Belgium
[3]Max Planck Institute for Marine Microbiology, Celsiusstraße 1, 28359 Bremen, Germany

Correspondence to: Ralf Hoffmann (ralf.hoffmann@awi.de)

Biogeosciences Discuss., https://doi.org/10.5194/bg-2017-537
Manuscript under review for journal Biogeosciences
Discussion started: 3 January 2018

Abstract

Arctic Ocean surface sea-ice conditions are linked with the deep sea benthic oxygen fluxes via a cascade of dependencies across ecosystem components like primary production, food supply, the activity of the benthic community, and their functions. Additionally, each of the ecosystem components is influenced by abiotic factors like light availability, temperature, water depth or grain size structure. In this study, we investigated the coupling between surface sea-ice conditions and deep-sea benthic remineralization processes through a cascade of dependencies in the Fram Strait. We measured sea-ice concentrations, nutrient profiles, different sediment compounds, benthic community parameters, and oxygen fluxes at 12 stations in the HAUSGARTEN area of the Fram Strait in water depth between 275–2500 m. Our investigations reveal that the Fram Strait is bisected in a permanently and highly sea-ice covered area and a seasonally and low sea-ice covered area, which both are long-lasting and stable. Within the Fram Strait ecosystem, sea-ice concentration and water depth are two independent abiotic factors, controlling the deep-sea benthos. Sea-ice concentration correlates well with the available food, water depth with the oxygen flux, and both abiotic factors correlate with the macrofauna biomass. However, in water depths >1500 m the influence of the surface sea-ice cover fades out and water depth effect becomes more dominant. Remineralisation across the Fram Strait is ~ 1 mmol C $m^{-2}d^{-1}$. Owing to the contrasting primary production pattern, our data indicate that the portion of newly produced carbon that is remineralised by the benthos is ~2.6 % in the seasonally low sea-ice covered Fram Strait but can be >15 % in the permanently high sea-ice covered Fram Strait. Furthermore, by comparing a permanently sea-ice covered area with a seasonally sea-ice covered area, we discuss a potential scenario for the deep-sea benthic ecosystem in the future Arctic Ocean, in which an increased surface primary production can lead to increasing benthic remineralisation in water depths <1500 m.

Biogeosciences Discuss., https://doi.org/10.5194/bg-2017-537
Manuscript under review for journal Biogeosciences
Discussion started: 3 January 2018

Copyright statement

The author transfers all copyright ownership of the manuscript entitled "Deep-sea benthic communities and oxygen fluxes in the Arctic Fram Strait controlled by sea-ice cover and water depth". The author warrants that the article is original, is not under consideration by another journal, and has not been previously published.

5

Biogeosciences Discuss., https://doi.org/10.5194/bg-2017-537
Manuscript under review for journal Biogeosciences
Discussion started: 3 January 2018

1 Introduction

The deep Arctic Ocean appears to have an enhanced coupling (relative to temperate and tropical waters) and therefore a strong linkage between surface waters and the benthos (Ambrose and Renaud, 1995; Graf et al., 1995; Grebmeier and Barry, 2007). For example, benthic deep-sea oxygen fluxes, representing the benthic ecosystem activity and the benthic remineralisation of carbon (Thamdrup and Canfield, 2000; Wenzhöfer and Glud, 2002; Smith et al., 2013), mirror surface primary production patterns (Graf et al., 1995; Wenzhöfer and Glud, 2002). However, each ecosystem components (primary production, benthic community and its activity, and benthic oxygen flux) depend on each other in the order as they are mentioned here and are additionally influenced by further factors. Primary production is influenced by a combination of abiotic factors like light intensity and light availability, advection, water stratification, sea surface temperature and nutrients (Bourgeois et al., 2017 and references therein). Benthic community parameters, like biomass, density, structure and functions of different fauna size classes, are influenced by sediment properties (Wheatcroft, 1992; Vanreusel et al., 1995), water depth, water temperature and food supply (Piepenburg et al., 1997; Flach et al., 2002; Smith et al., 2008). Benthic oxygen fluxes are known to depend on water depth (Wenzhöfer and Glud, 2002), benthic community biomass (Glud et al., 1994), and benthic community functions (Braeckman et al., 2010). Therefore, the ecosystem components primary production, benthic food supply, benthic community biomass, density and structure, benthic community functions and benthic oxygen flux are influenced by abiotic factors and additionally create a cascade of dependencies from the ocean's surface to and within the deep-sea benthos.

The occurrence of sea ice is an additional factor influencing primary production across the Arctic Ocean, as it ultimately alters the light availability (Arrigo et al., 2008; Bourgeois et al., 2017). As a consequence, the climate change induced alteration in the sea-ice cover influence biogeochemical cycles in the western Arctic (Harada, 2016). Further, a pan-arctic benthic oxygen flux model by Bourgeois et al. (2017) showed a better fit when benthic chlorophyll data, indicating surface primary production patterns, were taken into account. Boetius and Damm (1998) also found a good correlation between sea-ice cover, benthic chlorophyll and benthic carbon remineralisation in the Laptev Sea. However, microbial biomass, microbial activity, and labile organic matter supply are reported to be the key parameters controlling the benthic ecosystem in the dataset of Boetius and Damm (1998). Therefore, the strength of the linkage between the sea-ice cover and benthic remineralisation, even if often assumed as direct and strong, needs to be considered more carefully.

We were interested in the question, if we can link contrasting sea-ice conditions between the eastern and western Arctic Fram Strait (Soltwedel et al., 2005; Soltwedel et al., 2015; Spielhagen et al., 2015) with the deep-sea benthic oxygen fluxes over the cascade of dependencies of abiotic factors, primary production, benthic food supply, the benthic community, its activity and its functions. Our study provides sea-ice concentrations, sediment properties, biogenic sediment compounds, benthic community parameters, and benthic oxygen fluxes from 12 stations across the Arctic Fram Strait in water depths from 275 m to 2500 m. We hypothesise that the contrasting sea-ice conditions in the eastern and western Fram Strait (Soltwedel et al., 2005; Soltwedel et al., 2015; Spielhagen et al., 2015) lead to differences between parameters representing

the cascade of dependencies and result in contrasting benthic oxygen fluxes. Furthermore, our results allow us to estimate the portion of newly produced carbon that is remineralised by the benthic ecosystem. Furthermore, by comparing a permanently sea-ice covered area with a seasonally sea-ice covered area (western and eastern Fram Strait, respectively), we discuss a potential scenario for the deep-sea benthic ecosystem in the future Arctic Ocean.

2 Material and Methods

2.1 Study area and sample preparation

The Fram Strait is located in the northern Greenland Sea and forms a large passage (ca. 500 km wide) between northeast Greenland and the Svalbard archipelago (Fig. 1). It provides the only exchange route of intermediate and deep water masses between the Arctic and the Atlantic Ocean (Soltwedel et al., 2005; Forest et al., 2010). Two main currents influence the upper 300 m of Fram Strait waters (Manley, 1995): the East Greenland Current (EGC) and the West Spitsbergen Current (WSC). The EGC is located in the western Fram Strait and transports cold, less saline and nutrient poor (1 °C; <34.4) Arctic waters southward. In contrast, the WSC, located in the eastern Fram Strait, transports warmer, nutrient-rich Atlantic waters of higher salinity (>3 °C; >35) northward (Manley, 1995). About 22 % of the WSC is recirculated as the Return Atlantic Current (RAC). The remaining current bifurcates into the Svalbard Branch (SB; 33 %) and the Yermak Branch (YB; 45 %) following the Svalbard islands or flowing along the north-west flanks of the Yermak Plateau, respectively (Schauer, 2004). A high sea-ice cover is reported for the western Fram Strait and a low sea-ice cover for the eastern Fram Strait (Soltwedel et al., 2005; Soltwedel et al., 2015; Spielhagen et al., 2015). The sea-ice cover is relatively stable within the Fram Strait, even in the summer (Comiso et al., 2008; Soltwedel et al., 2015, https://www.pmel.noaa.gov/arctic-zone/detect/ice-seaice.shtml). However, the sea-ice age becomes younger by 0.6 years per decade (Krumpen et al., 2015), which goes along with a decrease in the sea-ice thickness (Renner et al., 2014; Krumpen et al., 2015).

Two sampling campaigns were carried out at the long-term ecology research observatory HAUSGARTEN (Soltwedel et al., 2005) in the Fram Strait with RV *Polarstern*, expedition "PS85" from 6/6–3/7/2014 and expedition "PS93.2" from 22/7–15/8/2015. Samples were taken at five stations at the East Greenland continental slope (EG area) and at seven stations at the West Spitsbergen continental slope (WS area). Four stations in each area form a bathymetric transect roughly along the 79° latitude, namely EG I, EG II, EG III, and EG IV in the EG area and HG I, HG II, HG III, and HG IV in the WS area, both with water depths between 1000–2500 m (Fig. 1, Table 1). Further, four additional stations were sampled; "EG V" in the EG area and "N5", "SV IV" and "SV I" in the WS area. These stations are not located along the 79° latitude and were taken as they allow a deeper discussion of our hypothesis. The station EG IV includes two sites which are located < 2 km from each other (Table 1) and the stations HG I, HG II, HG III, and HG IV were sampled during both sampling years, 2014 and 2015.

Sediment sampling was performed by using a multiple corer (MUC) with eight tubes and autonomous benthic lander systems (Reimers, 1987; Glud et al., 1994) equipped with three benthic chambers and a sediment profiler with oxygen

sensors. Water sampling in different water depths was performed, using a SBE32 rosette water sampler equipped with 24 Niskin-type sample bottles (12 L). A detailed list of the number of used samples per station for the determination of different parameters is given in Table S1 in the supplements.

2.2 Sea ice data and pelagic nutrient profiles

Daily sea ice concentrations for each of the analysed stations were obtained from the Center for Satellite Exploitation and Research (CERSAT) at the Institut Français de Recherche pour l'Exploitation de la Mer (IFREMER), France (Ezraty et al., 2007) and were previously published (Krumpen, 2017), except for station EG V. Sea-ice concentration was calculated based on the ARTIST Sea Ice (ASI) algorithm developed at the University of Bremen, Germany (Spreen et al., 2008). The data used within this study covers the period from 01/09/2001 till 31/08/2015 (long-term data) with a 12.5 x 12.5 km² spatial resolution around the station. Data points with a value of >100 % were omitted as such a value indicates a mismeasurement. A subset for short-term examinations was extracted, which includes the time a year before sampling. This was the period 01/07/2013–30/06/2014 for stations sampled in 2014 and 01/08/2014–31/07/2015 for stations sampled in 2015. From each dataset (long-term and short-term) the sea-ice cover and the percentage of days with sea-ice cover were extracted.

Water samples were used to measure nitrate and phosphate concentrations. The measurement was performed with a standard photometric method using a Technicon TRAACS 800 continuous flow autoanalyser (Technicon Corporation). A daily calibration of the autoanalyser was executed using NIST-standards (Merck, certified reference material: NMIJ CRM7602-a). The data were previously published by Graeve and Ludwichowski (2017).

2.3 Sediment compounds and properties

Various biogenic sediment compounds including grain size, water content, chlorophyll a (Chl *a*) and phaeopigment concentrations (Phaeo), total organic carbon (TOC), phospholipids, proteins, organic matter, and the bacterial enzymatic turnover rate (FDA) as bacterial activity proxy were determined from the sediments sampled by the MUC and chambers of the autonomous benthic lander system. Generally, three pseudo-replicates from each MUC (sampled from different sediment cores, inner MUC tube diameter = 9.5 cm) were taken. Sediment samples of the uppermost five sediment centimetres were taken by means of syringes with cut-off ends (1.17 / 3.14 cm² cross-sectional area). Samples for FDA, Chl *a*, and Phaeo were immediately analysed on board. All other samples were shock frosted at -80°C and stored at -20°C until they were analysed at the home laboratory. Sediment samples, taken by the benthic chambers of the autonomous lander system, were treated similarly.

The grain size partitions were determined with a Malvern Mastersizer 2000G, hydro version 5.40. The Mastersizer utilizes a laser diffraction method and has a measuring range of 0.02–2000 µm. The water content of the sediment was determined by the difference in weight of the sediment before and after drying at 105°C. The bioavailability of phytodetritus at the seafloor was assessed by analysing sediment bound Chl *a* and Phaeopigments. Chloroplastic pigments were extracted in 90 % acetone and measured with a TURNER fluorometer (Shuman and Lorenzen, 1975). The bulk of pigments (Chl *a*

plus Phaeo) are termed chloroplastic pigment equivalents (CPE) after Thiel (1978). Additionally, the ratios of Chl *a* to Phaeo, as an indicator of the relative age of the food, and the Chl *a* to CPE (% Chl *a*), a quality indicator of the labile organic matter, was calculated. The percentage of the TOC was measured by combustion using an ELTRA CS2000 with infrared cells. To indicate the quantity of cell wall material, phospholipids were measured following Findlay et al. (1989) with modifications after Boetius and Lochte (1994). Particulate proteins, defined as γ-globulin equivalents (Greiser and Faubel, 1988), were measured to differentiate between living organisms and detrital organic matter in the sediments. Hereafter, particulate proteins will be referred to only as proteins. The organic matter was determined as ash free dry weight after combustion (2 h, 500°C). Bacterial enzymatic turnover rates were calculated using the fluorogenic substrate fluorescein-di-acetate (FDA) as an indicator of the potential hydrolytic activity of bacteria (Köster et al. 1991).

2.4 Benthic community parameters

For the bacterial density determination, sediment subsamples were taken with modified syringes (1.17 cm² cross-sectional area) from MUC recovered sediment cores after oxygen flux measurements were performed and from benthic chambers. The first centimetre of each sample was stored in a 2 % filtered formalin solution at 4 °C. The acridine orange direct count (AODC) method (Hobbie et al., 1977) was used to stain bacteria in the subsamples and subsequently bacteria were counted with a microscope (Axioskop 50, Zeiss) under UV–light (CQ-HXP-120, LEj, Germany).

For the determination of the meiofauna density and identification of meiofauna taxa, sediment subsamples were taken with modified syringes (3.14 cm² cross-sectional area) from MUC recovered sediment cores after oxygen flux measurements were performed and from benthic chambers. The first centimetre of each sample was stored in borax buffered 4 % formaldehyde solution at 4 °C. The samples were sieved over a 1000 µm and 32 µm mesh. Both fractions were centrifuged three times in a colloidal silica solution (Ludox TM-50) with a density of 1.18 g/cm³ and stained with Rose Bengal (Heip et al., 1985). Afterwards, the taxa were identified and counted. Foraminifera are not considered, as the extraction efficiency of Ludox for different groups of foraminifera is insufficient for a quantitative assessment of the group. Therefore, only metazoan meiofauna is recorded and hereinafter the use of the term meiofauna refers only to metazoan meiofauna organisms.

After taking subsamples for bacteria and meiofauna densities, the remaining sediment from MUC recovered sediment cores and from the benthic chambers was used for macrofauna taxonomical identification, and density and biomass determination. For these macrofauna analyses only the 0–5 cm horizon from MUC sediment cores and the entire remaining sediment from the benthic chambers was used, sieved over a 500 µm mesh and stored in borax buffered 4 % formaldehyde and stained with Rose Bengal (Heip et al., 1985). Afterwards, macrofauna taxa were identified to the highest taxonomic level, counted and weighted (blotted wet weight).

From the macrofauna density (*Ai*) and biomass (*Bi*), together with a mobility score (*Mi*) and sediment reworking score (*Ri*) of each taxon, the community bioturbation potential (*BPc*) was calculated following Queirós et al. (2013, Eq. (5)):

Biogeosciences Discuss., https://doi.org/10.5194/bg-2017-537
Manuscript under review for journal Biogeosciences
Discussion started: 3 January 2018

$$BP_c = \sum_{i=1}^{n} \sqrt{B_i / A_i} \times A_i \times M_i \times R_i \quad (5)$$

in which i displays the specific taxon in the sample. This index represents the bioturbation potential of the benthic macrofauna community.

2.5 Oxygen and bromide fluxes

Immediately after the retrieval of sediment cores by the MUC, a part of the overlying water was removed and stored separately. At least 10 cm overlying water remained in the cores. The sediment of each core was carefully pushed upwards without disturbing the surface sediment layer until the sediment–water interface (SWI) was at a distance of around 10 cm from the upper edge of the core. A magnetic stirrer was added to the overlying water. In this position, the sediment cores were stored in a water bath at in situ temperature (-0.75°C) until the start of the oxygen flux measurements.

For the determination of the ex situ diffusive oxygen uptake (DOU) at least two oxygen microprofiles per sediment core were measured simultaneously within 2 h after sampling with a vertical resolution of 100 µm. The profiling was performed by oxygen optical microsensors (OXR50, Pyroscience, Aachen, Germany) with a tip size of 50 µm in diameter, a response time of <2 s and an accuracy of ±0.02 %, calibrated with a two-point calibration using air saturated and anoxic waters (by adding sodium dithionite). The overlying water in the MUC cores was magnetically stirred and the water surface was gently streamed with a soft air stream during the profiling. The maximum penetration depth of the sensors during ex situ profiling was 42 mm. For in situ DOU determination autonomous landers were used (Reimers, 1987; Glud et al., 1994; Glud, 2008). The profiling unit was equipped with electrochemical oxygen microsensors (custom made after Revsbech (1989)) and calibrated with a two-point calibration. As the first calibration point, the bottom water oxygen concentration (water sample were taken by Niskin bottle), estimated by Winkler titration (Winkler, 1888), was used. As the second calibration point, the sensor signal in the anoxic zone of the sediment (when reached) or the sensor signal in an anoxic solution of sodium dithionite was used. The measurements started three hours after the deployment of the autonomous lander, allowing resuspended sediment to settle on beforehand. Profiling was performed with a depth resolution of 100 µm. The maximum penetration depth of the sensors during in situ profiling was 180 mm. Running average smoothed oxygen profiles from ex situ and in situ approaches were used to calculate the DOU rates across the SWI using Fick's first law (Eq. (1)):

$$DOU = -D_s \times \left[\frac{\delta O_2}{\delta z}\right]_{z=0}, \quad (1)$$

in which *Ds* is the molecular diffusion coefficient of oxygen in sediments at in situ temperature and salinity, and $\left[\frac{\delta O_2}{\delta z}\right]_{z=0}$ is the oxygen gradient at the SWI calculated by linear regression from the first alteration in the oxygen concentration profile across a maximum depth of 1 mm. *Ds* was calculated following Schulz (2006) as D/θ^2, with D as the molecular diffusion coefficient of oxygen in water after Li and Gregory (1974), and θ^2 as $1-ln(\varphi^2)$ (Boudreau, 1997). The sediment porosity φ was calculated following the equation of Burdige (2006, Eq. (2)):

$$\varphi = \frac{m_w/\rho_w}{m_w/\rho_w + (m_d - (S \times m_w))/\rho_s}, \quad (2)$$

In this equation, *mw* is the mass of evaporated water, ρw is the density of the evaporated water, *md* is the mass of dried sediment plus salt, *S* is the salinity of the overlying water and ρs is the density of deep-sea sediment (2.66 g cm^{-3}, after Burdige, (2006)). To calculate *mw*, ρw, and *md*, the weight loss of wet sediment samples was measured by weighing wet samples, drying them overnight at 70 °C, weigh them again, dry the sample for 1 h at 70 °C and weigh them a second time. This procedure was repeated until the weights of the two dried samples differ not more than 0.05 %.

For ex situ total oxygen uptake (TOU) measurements, sediment cores were used after oxygen microprofiling (see upper paragraph in this section). The sediment cores were closed airtight with no air bubbles in the overlying water. The distance between the SWI and the edge of the lid was measured for volume calculations of the overlying water. An optical oxygen microsensor (Pyroscience, Aachen, Germany) with a tip size diameter of 50 µm was installed in the lid, allowing a continuous measurement of the oxygen concentration in the overlying water. The sediment cores were incubated in darkness for >40 h and the overlying water was kept homogenised by rotating magnets over that period. For in situ TOU measurements, benthic chambers (K/MT 110, KUM, Kiel, Germany) with an inner dimension of 20x20 cm were used. These chambers were pushed into the sediment and thereby enclosed a sediment volume of approximately 8 L and an overlying water volume of approximately 2–3 L. The oxygen concentration was measured in the overlying water continuously with an Aanderaa optode (4330, Aanderaa Instruments, Norway, two-point calibrated as described in the upper section) over an incubation period of 20–48 h. During the measurement, the overlying water was kept homogenised by a stirring cross at the inner top of the chamber. TOU from both ex situ sediment core and in situ benthic chamber incubations were calculated using Eq. (3):

$$TOU = \frac{\delta O_2 \times V}{\delta t \times A}, \quad (3)$$

in which $\delta O2$, δt, *V* and *A* represent the difference in oxygen concentration, the difference in time, the volume of the overlying water and the enclosed surface area, respectively.

The oxygen fluxes were converted to carbon equivalents (C-DOU and C-TOU) by applying the Redfield ratio (C:O = 106:138; Redfield (1934)) in order to compare them to the carbon fixed by primary production. Modifications, as suggested by Takahashi et al. (1985) and Anderson and Sarmiento (1994), would result only in minor changes of <10 % in the benthic carbon flux.

To assess the exchange of solutes across the SWI, which results from molecular diffusion, physical advection, and faunal ventilation activities, sodium bromide (NaBr) was added to the removed overlying water of the sediment cores to create a NaBr–solution of similar density as seawater (1028 g/L). The NaBr–solution was added to the sediment cores before the TOU incubation started. Three subsamples of water were taken during the incubation at three different times (t_0, t_1, t_2) and stored at 4 °C. Removed water volume of the subsampling at t_1 was replaced with the NaBr–seawater solution. The bromide concentrations were measured using ion chromatography. The dilution of the t_2–sample, due to the sampling procedure, was corrected by the known bromide concentration in the removed and the added water. The bromide exchange is represented by the bromide flux, calculated using the Eq. (4):

Biogeosciences Discuss., https://doi.org/10.5194/bg-2017-537
Manuscript under review for journal Biogeosciences
Discussion started: 3 January 2018

$$Bromide\ flux = \left(\frac{\delta Bromide\ concentration \times V}{\delta t \times A}\right), \quad (4)$$

in which *δBromide concentration*, *δt*, *V* and *A* represent the difference in bromide concentration, the difference in time, the volume of the overlying water and the enclosed surface area, respectively.

2.6 Data analyses

The analysed data sets were obtained during two subsequent years (Table 1). To test whether there is a significant offset between sampling years, a principal component analysis (PCA) was performed on standardised (x to zero mean and unit variance) abiotic parameters (year, water depth, sea ice cover, percentage of days with sea ice cover, the portion of grain size >63 µm, median grain size) and all sediment compounds and property parameters from the 0-1cm sediment horizon, as it was the most complete data set. Additionally, a non–parametric Wilcoxon signed rank sum test was performed on station specific mean values of both years on water content, TOC, organic matter, Chl *a*, Phaeo, protein, phospholipids, FDA, DOU and TOU following Cathalot et al. (2015). Both tests were performed only on data of stations that were sampled in both 2014 and 2015.

To identify the most important parameters influencing the benthic Fram Strait ecosystem, a second PCA was performed on standardised (x to zero mean and unit variance) ex situ mean values of abiotic parameters (water depth, sea-ice cover, the portion of grain size >63 µm, water content), biogenic compound parameters (Chl *a*, TOC, organic matter), oxygen fluxes (DOU, TOU), the benthic community (bacterial density, macrofauna biomass), and macrofauna mediated environmental functions (bromide exchange, *BPc*). All other parameters were excluded from the PCA as they correlated strongly (correlation >0.74, Pearson correlation, Supplement Table S2) with one of the mentioned parameters used for the PCA. This procedure results in a more resilient outcome of the PCA. For station EG II no bromide exchange value could be calculated because the residuals over the slope did not follow a Gaussian distribution. Nevertheless, in order to perform the PCA, the mean value of all EG stations and N5 was assumed to represent the bromide exchange at EG II. Furthermore, due to its exceptional low water depth, the values from station SV I were also excluded from the PCA. For further insights and descriptions of the usage and interpretation of a PCA visualization, the reader is referred to Buttigieg and Ramette (2014).

Water depth and sea ice have a profound impact on benthic oxygen fluxes (Wenzhöfer and Glud, 2002; Harada, 2016). To investigate the influence of water depth and sea ice in our data, the stations were merged into two sea-ice cover categories. First, a“high sea-ice concentration” area (HSC), which include stations with a short-term (a year before sampling) mean sea-ice concentrations of ≥ 30 %. Second, a “low sea-ice concentration” area (LSC), which include stations with a short-term (a year before sampling) mean sea-ice concentrations of <30 %. Regression analysis was used to test the water depth dependence of sediment compounds and property parameters, the benthic community parameters, the oxygen fluxes, and parameters of the macrofauna mediated environmental functions within the HSC and LSC categories. If the residuals over the slope did not follow the Gaussian distribution (tested with a Shapiro–Wilk test), values were transformed, either by square root or logarithmic transformation. Individual values that failed due to technical failure or mismeasurements were

removed before statistical analyses. For all above mentioned statistical treatments, R Statistical Software (version 3.4.0) was used.

Analyses of the multivariate meio- and macrofauna community structure were based on square root transformed density and biomass data of sediment core replicates. Non–metric multidimensional scaling (MDS, (Kruskal, 1964)) and hierarchical cluster analysis with group average clustering were used to present the multivariate similarities between samples based on Bray–Curtis similarity. Significant multivariate differences between pre-defined group structures within the meio- and macrofaunal data were tested by the ANOSIM procedure (ANalysis Of SIMilarity) based on Clarke's R statistic (Clarke and Warwick, 1994) with 9999 permutations. The SIMPER (SIMilarity PERcentage) routine was applied to determine the contribution of certain meio- and macrofauna taxa towards the discrimination between sea-ice cover categories and water depth categories. Differences between HSC, LSC and water depth regarding macrofauna density and macrofauna biomass were examined using a two-way crossed PERMANOVA (PERMANOVA+ for PRIMER; Anderson, 2005; Anderson et al., 2007) analysis with "site" (levels "HSC" and "LSC") or "water depth" (levels:1000, 1500, 2000, 2500 m) as fixed factors. The significance level was set at 0.05. Significant main PERMANOVA tests were followed by pairwise PERMANOVA tests. Permutational P-values (PPERM) were interpreted when the number of unique permutations was >100; alternatively, Monte Carlo P-values (PMC) were considered. Bray–Curtis similarity was used to construct resemblance matrices. Data were standardised and fourth–root transformed (to down weigh the importance of the most dominant taxa) prior to the construction of resemblance matrices. The station SV I and the in situ stations HG I Lander and HG IV Lander were excluded from these test, owing to its shallow location (SV I) and different sampling device (benthic chambers insteadt of MUC). All analyses of multivariate community structure were performed using the routines implemented in PRIMER vers. 6.1.15 (Clarke and Gorley, 2006; Anderson et al., 2007). Results are expressed as means ± standard deviation.

3 Results

3.1 Short- and long-term sea ice concentration comparison between the EG and WS area

Short-term and long-term data of the mean sea-ice concentrations and the percentage of sea-ice covered days were in a comparable range (Table 2, Supplement Table S3). Both parameters in both datasets decrease from west to east with a sharp drop between N5 and HG IV (Table 2 for short-term data, Fig. 2 for long-term data). Therefore, the categorisation into a high sea-ice covered area (HSC) and a low sea-ice covered area (LSC) was introduced. The HSC includes all East Greenland stations (EG I–V) and the most northern West Spitzbergen station N5, while the LSC includes the remaining West Spitzbergen stations (HG I–IV, SV I, and SV IV).

Generally, the east Greenland stations showed the highest sea ice concentration, as expected due to the influence of the East Greenland current. The short-term sea-ice concentration in the EG area was highest at EG I with 82 ± 20 % (n=364) and lowest at EG V with 56 ± 34 % (n=364). In the WS area, sea-ice concentration was highest at N5 with 40 ± 31 % (n=365) and lowest at SV IV with 0.1 ± 2 % (n=365). The percentage of days, which showed sea-ice cover, during the short-

term period in the EG area was highest at EG I, EG II and EG III (each with 100 %) and lowest at EG V (93 %). In the WS area the percentage of days, which showed sea-ice cover, during the short-term period was highest at N5 (82 %) and lowest at SV IV (>0.1%, Table 2). These patterns were also visible in long-term sea-ice concentration and the percentage of sea-ice covered days (Supplement Table S3).

3.2 Water column nutrient profiles, sediment properties and benthic biogenic compounds in the EG and WS area

Nitrate and phosphate concentrations increased with increasing water depth. In general, both nutrients showed higher concentrations in the WS area than in the EG area. However, at the surface, nitrate concentrations were higher in the EG area (Supplement Fig. S1)

Values for all sediment properties and biogenic compounds at the deeper stations (>1500 m) in the EG and WS area were in the same range. In contrast, shallow stations (≤ 1500 m) of the WS area showed higher values compared to shallow stations of the EG area (Table 2). This leads to higher variances in the WS area for most of the determined parameters (Fig. 3). The portion of sediment grain size >63 µm, median grain size, water content, and porosity showed a similar range of variances for the EG and the WS area and median values of the portion of sediment grain size >63 µm and the median grain size are highly comparable between both areas (Fig. 3.). Nevertheless, values of water content (59 ± 8 % in the WS area as opposed to 47 ± 9 % in the EG area) and porosity (0.83 ± 0.06 in the WS area as opposed to 0.73 ± 0.07 in the EG area) differ between the WS and EG area. It indicates sediment properties are a potentially important factor that maybe influence benthic oxygen fluxes. Median values for each pelagic food supply indicating parameter in the sediment (Chl *a*, Phaeo, and CPE) were four times higher and showed greater variances in the WS area than in the EG area. Values for parameters indicating food quality (Chl *a*–CPE ratio) and relative age of food (Chl *a*–Phaeo ratio) were in the same range for the EG and WS area. The WS area showed higher TOC, organic matter, protein and lipid contents than the EG area and as well had higher variances in the WS area compared to the EG area. However, the bacterial enzymatic activity (FDA) and its variances were similar between the EG and the WS area (Fig. 3). This indicates contrasting food supply quantities between the EG and the WS area, while the food quality is similar.

3.3 Differences between benthic communities and community functions in the EG and WS area

Overall, 17 meiofauna taxa and 18 macrofauna taxa were identified (Supplement Tables S4, S5, S6). The meiofauna density was dominated by nematodes (86 %), the only taxon present at each station. Crustaceans were the second most dominant group with 4.5 % nauplii and 3.5 % Copepoda. The macrofauna density was dominated by polychaetes (40 %), followed by Copepoda (26 %), and Nematoda (12 %). Polychaetes (57 %) also dominated the macrofauna biomass, followed by Bivalvia (16 %) and Porifera (14 %). The mean values of the benthic community parameters meiofauna density, macrofauna density and macrofauna biomass were 1.5 times, 4.6 times and 2.5 times higher in the WS area than in the EG area, respectively, and showed greater variances in the WS area. Contrasting, the bacterial density was comparable between the EG and WS area, but showed a greater variance in the WS area (Fig. 3).

The solute exchange across the SWI, represented by the bromide flux, and the community bioturbation potential, represented by the *BPc*, were 1.2 times and 2.9 times higher in the WS area than in the EG area, respectively, and showed higher variances in the WS area (Fig. 3). This indicates that the benthic macrofauna community in the WS area is able to rework the sediment stronger than the benthic macrofauna community in the EG area. It needs to be mentioned that bromide flux incubations were performed on 40 sediment cores. Measurements from 13 sediment cores were omitted, as either the calculations revealed a positive flux or the residuals were not homogenously distributed across the decreasing slope of the bromide concentration over time or slopes were not significantly different from zero.

3.4 Benthic activity and remineralisation

All oxygen profiles showed decreasing oxygen concentrations across the SWI (Supplement Fig. S2) and varying steepnesses of oxygen gradients between profiles and across various stations. Further, all sediment core incubations resulted in decreasing oxygen concentrations in the overlying water, with varying steepnesses between sediment cores and across various stations. In general, DOU and TOU values in the EG and WS area were in a similar range (Fig. 3).

The mean DOU in the EG area ranged between 0.4 ± 0.1 mmol O_2 $m^{-2}d^{-1}$ (n=10) at EG V and 1.0 ± 0.1 (n=10) mmol O_2 $m^{-2}d^{-1}$at EG II. In the WS area, DOUs at stations within the same water depth range as the EG stations ranged between 0.5 ± 0.2 mmol O_2 $m^{-2}d^{-1}$ (n=8) at HG IV and 2.1 ± 0.6 (n=8) mmol O_2 $m^{-2}d^{-1}$ at SV IV. At the shallow station SV I the DOU reached 3.0 ± 1.7 mmol O_2 $m^{-2}d^{-1}$ (n=6, Table 2). The mean TOU in the EG area ranged between 0.9 ± 0.3 mmol O_2 $m^{-2}d^{-1}$ (n=2) at EG I and 1.6 (n=1) mmol O_2 $m^{-2}d^{-1}$ at EG II. Similar mean TOU values were measured in the WS area, at stations within the same water depth range as the EG stations. TOU values ranged between 0.5 ± 0.2 mmol O_2 $m^{-2}d^{-1}$ (n=5) at HG IV Lander and 1.9 ± 0.6 (n=5) mmol O_2 $m^{-2}d^{-1}$ at HG I. At the shallow SV I station TOU reached 5.1 ± 0.3 mmol O_2 $m^{-2}d^{-1}$ (n=3, Table 2). The mean DOU/TOU ratio across the entire Fram Strait was 0.79 ± 0.30, with 0.63 ± 0.22 in the EG area and 0.92 ± 0.30 in the WS area which indicates bacterial activity and bacterial remineralisation as the major oxygen consumer. In the EG area, DOU values showed no correlation with water depth, while in the WS area the correlation of DOU with water depth was significant and showed greater variation (Fig. 4). Contrastingly, TOU values in the EG and in the WS areas showed no correlation with water depth, but again, the variations of the TOU values were higher in the WS area (Fig. 4). DOU and TOU values were converted into C-DOU and C-TOU and are listed in Table 2.

3.5 Relations of the benthic community, its remineralisation activity, and environmental parameters

The PCA which includes only abiotic parameters (year, water depth, sea ice cover, the percentage of days with sea ice cover, portion of grain size >63 µm, and median grain size) and biogenic compounds of the first sediment centimetre (Chl *a*, Phaeo, CPE, TOC, organic matter, lipids, and proteins) revealed differences between the sampling years 2014 and 2015 (Supplement Fig. S3). The difference occurred only in the second dimension, which explains 15.4 % of the variability and is mostly influenced by the parameters Phaeo and CPE (Supplement Table S7). These differences are probably a result of the different sampling periods (June in 2014 and end of July/beginning of August 2015), resulting in different Phaeo and CPE

concentrations. The non-parametric Wilcoxon signed rank sum test of the station specific mean values revealed no differences ($p > 0.05$) for any of the parameters between the sampling years. Furthermore, Henson et al. (2016) showed that it takes at least 15 years of continuous data to proof temporal trends in ocean biogeochemistry; and even longer in high latitudinal areas. Therefore, it is more likely that statistically revealed differences between sampling years are presenting spatial variability rather than time-related differences. Therefore, the data from stations sampled in 2014 and 2015 were merged to focus on spatial patterns.

The PCA on station specific, ex situ obtained mean values (Fig. 5) revealed that water depth was positively correlated with median grain size and negatively correlated with the DOU, the TOU, bacterial density, and the *BPc*. Sea-ice concentration was negatively correlated with the porosity, Chl *a*, TOC, organic matter, and solute exchange. Similarly, macrofauna biomass was negatively correlated with both, water depth and sea-ice concentration. Additionally, EG I, EG II, and EG III were strongly influenced by the sea-ice cover, while station EG IV was slightly more influenced by the factor water depth. The two dimensions in the plot together explained 66.9 % of the total variability of the data.

Across the HSC area, DOU (Fig. 4) and TOU were not linearly dependent on water depth (Supplement Table S8). The same was found for the water content, FDA, meiofauna and macrofauna densities, macrofauna biomass, and the solute exchange across the SWI. Otherwise, the fraction of sand in the sediment (% of grain size >63 µm), Phaeo, CPE, the Chl *a*–Phaeo ratio, the Chl *a*–CPE ratio, and lipids were positively linearly dependent on water depth across the HSC area and the BPc was negatively linearly dependent on water depth. Across the LSC area, the DOU was negatively linearly dependent on water depth, as well as sediment water content, Chl *a*, Phaeo, CPE, FDA, bacteria density and bioturbation potential. Contrastingly, TOU, Chl *a*–Phaeo ratio, protein, meio- and macrofauna densities, macrofauna biomass, and the solute exchange were not water depth dependent across the LSC area. Within both sea-ice categories HSC and LSC, no linear water depth dependencies were found for median grain size, TOC, and organic matter as the residuals over the slopes did not follow the Gaussian distribution. This also applied for Chl *a*, protein, and bacteria density across the HSC area and for the portion of grain size >63 µm, the Chl *a*–CPE ratio, and lipids across the LSC area (Supplement Table S8).

The ANOSIM (Global $R = 0.122$, $p = 0.063$) and SIMPER (33 % dissimilarity) routine revealed no differences between the HSC and LSC area regarding the meiofauna community based on density (Table 3). Regarding macrofauna communities based on density (Global $R = 0.257$, $p = 0.007$) and biomass (Global $R = 0.238$, $p = 0.003$), the ANOSIM revealed significant differences between the HSC and LSC area. SIMPER routine results indicated dissimilarities of 56 % for the macrofauna density and 76 % for the macrofauna biomass between the HSC and LSC areas. The taxa contributing most to the average similarity within and to the average dissimilarity between the HSC and LSC area are given in Supplement Table S9. The ANOSIM results for water depth groups showed that bathymetry could at least explain partly the dissimilarity in meiofauna communities based on density (Global $R=0.219$; $P=0.01$). The SIMPER analysis, however, showed that the observed differences in meiofauna density regarding water depth are mainly due to the marked difference between the shallowest station (SV I at 275 m) and all other stations deeper than 1000 m (dissimilarity > 50 %, Supplement Table S10). ANOSIM results for macrofauna communities based on density (Global $R = 0.2$, $p = 0.008$) and biomass (Global $R = 0.346$,

p = 0.0001) revealed significant differences between water depth categories with >50 % dissimilarity between all water depth categories for macrofauna density (except between 1000 m and 1500 m) and macrofauna biomass (SIMPER, Supplement Table S10). Further, the two-way crossed PERMANOVA revealed that the sea-ice coverage (LSC and HSC) explains a significant (p = 0.008) portion of the macrofauna density variability, while the portion explained by water depth (p = 0.06) and by the interaction of sea-ice cover and water depth (p = 0.09) was not significant (Supplement Table S11). However, the results of the pairwise test showed that only the neighbouring water depth classes 1000 m and 1500 m showed no significant differences (p = 0.45) while all other pairwise comparisons showed significant differences between water depths (Supplement Table S12). For macrofauna biomass the two-way crossed PERMANOVA revealed that the interaction of sea-ice cover and water depth explains a significant (p = 0.034) portion of the macrofauna biomass variability, while the portion explained by the sea-ice cover categories (p = 0.051) and by water depth (p = 0.058) was not significant (Supplement Table S11). The results of the pairwise test showed that only the water depth classes 1000 m and 2500 m showed significant differences (p = 0.0187) while all other pairwise comparisons showed no significant differences between water depths (Supplement Table S12).

4 Discussion

4.1 Linking contrasting sea-ice conditions with benthic oxygen fluxes

The main question of this study was to link contrasting sea-ice conditions within the Arctic Fram Strait (Soltwedel et al., 2005; Soltwedel et al., 2015; Spielhagen et al., 2015) with the deep-sea benthic oxygen fluxes over a cascade of dependencies. Our results document two contrasting sea-ice concentration regimes in the Fram Strait with a high sea-ice cover in the western Fram Strait and a low sea-ice cover in the eastern Fram Strait (Table 2, Fig. 2). This is similar to sea-ice concentration snapshot observations by Schewe and Soltwedel (2003) and satellite observations of Krumpen et al. (2015). The observed pattern can be explained by the two major current systems present in the Fram Strait (Schauer, 2004), the EGC transporting cold water and sea ice from the central Arctic Ocean southwards into the EG area and the WSC transporting warmer, sea-ice free water from the Atlantic Ocean northwards into the WS area (Manley, 1995). If there is a strong link between sea-ice conditions and deep-sea benthic oxygen fluxes, we expected contrasting primary production, benthic food supply, benthic community parameters and benthic oxygen fluxes between the EG and the WS area.

Our results indeed indicate a potentially higher primary production in the WS area, compared to the EG area. The general nutrient distribution differs between the EG and WS area, with higher nitrate and phosphate concentrations in the WS area. The nutrient distribution follows the sea-ice pattern and is also mainly influenced by the general current system in the Fram Strait, as the EGC transports water masses with lower nutrient concentrations and the WSC water masses with higher nutrient concentrations (Manley, 1995). Therefore, the initial conditions for primary production in the Fram Strait would support higher primary production in the WS area, as more light (owing less sea ice) and more nutrients are available. As the sampling was performed in June 2014 and July/August 2015, it is very likely that the season of new production,

which usually starts in May (Cherkasheva et al., 2014), had already ended. This explains the low nitrate concentration values within the first 20–40 m water depth in the EG and WS area (Supplement Fig. S1). Interestingly, higher phosphate concentration values were found in the EG area compared to the WS area within the first 20–40 m water depth, which is contrary to the observed phosphate distribution pattern over the entire water depth. It indicates that primary production in the EG area is nitrate limited, similar to the permanently sea-ice covered central Arctic Ocean (Tremblay et al., 2012, Fernández-Méndez et al., 2015). The pattern of contrasts between the EG and WS area continued in the benthic food supply, with generally higher values of benthic food supply representing parameters in the WS area compared to the EG area (Fig. 3) and indicated by the negative correlation of the sea-ice concentration with Chl *a*, TOC and organic matter (Fig. 5), which also was found by Boetius and Damm (1998) for the continental margin of the Laptev Sea.

Continuing the cascade of dependencies, benthic community biomass and density should follow the same pattern as the sea ice at the surface and the benthic food supply parameters. There are differences between the EG and WS area regarding meiofauna density, macrofauna density and macrofauna biomass (Fig. 3). However, the comparable angles between the macrofauna–water depth arrow and the macrofauna–sea-ice concentration arrow in figure 5 indicated that macrofauna biomass is also influenced by water depth and not only by the sea-ice cover. It needs to be mentioned that the term "macrofauna biomass" used in figure 5, also represents the macrofauna density, meiofauna biomass, and meiofauna density (Supplement Table S2) and therefore the entire benthic community. Furthermore, when taking both abiotic factors (sea ice and water depth) into account, the contrasting water depth–macrofauna density relationship between high and low sea-ice covered areas became visible (Supplement Fig. S4). Additionally, our data reveal significant differences in the macrofauna community structure based on sea-ice cover categories (Table 3) and water depth (Supplement Table S10) and on macrofauna density and macrofauna biomass (Supplement Table S11 and S12). Thereby, the PERMANOVA confirm the influence of water depth on the macrofauna community and indicate that water depth is a considerable factor besides the sea-ice cover. Consequently, in the low sea-ice covered WS area macrofauna is mainly influenced by the abiotic factor water depth (Soltwedel et al., 2015), while in the highly sea-ice covered EG area the abiotic factor sea-ice cover co-act or even replace water depth as most influencing abiotic factor.

Continuing the cascade of dependencies to the benthic activity, represented by the oxygen flux; we did not reveal a correlation of oxygen fluxes with sea-ice concentrations or benthic food supply, only with water depth (Fig. 5). This is contrasting to our expectations and to findings of Boetius and Damm (1998). However, a PCA only shows correlations but do not test significances of these relationships within it. Therefore, we test the significance of the correlation of water depth with DOU within the sea-ice concentration categories HSC and LSC, which reveals a slightly different pattern. The regression of the DOU on water depth is only significant in the LSC category, but not in the HSC (Fig. 4). Therefore, the bacterial benthic activity, which makes up ~ 80 % of the TOU (Table 2), depends on water depth in low sea-ice covered areas, but not in the highly sea-ice covered EG area. To test, if this pattern is also true for the macro- and meiofauna activity,

represented by the fauna oxygen uptake (= TOU minus DOU), we assessed as not reliable owing a lower reproducibility of TOU values.

In the Fram Strait, sea-ice cover and water depth are totally independent abiotic factors influencing the benthic ecosystem and thereby the cascade of dependencies between ecosystem components. The sea-ice cover is directly linked to the primary production and to the benthic food supply. The deep-sea benthic community is influenced also by water depth, which represents a proceeding degradation state of settling organic material towards the sea floor (Belcher et al., 2016). This fits the findings, that labile organic matter is the most important factor determining Arctic deep-sea benthic communities (Grebmeier et al., 1988; Klages et al., 2004). Regarding the benthic activity, the Fram Strait is bisectional: water depth independent in the highly sea-ice covered western Fram Strait and water depth dependent in the low sea-ice covered eastern Fram Strait.

4.2 Primary production and benthic remineralisation in the Fram Strait

Our oxygen fluxes within the HSC and LSC categories are comparable to earlier findings within the Fram Strait by Sauter et al. (2001) and Cathalot et al. (2015) and also by findings of Boetius and Damm (1998) for the continental margin of the Laptev Sea, but slightly lower than the modelled results by Bourgeois et al. (2017, Fig. 6).The total benthic carbon remineralisation across the entire Fram Strait is ~1 mmol C $m^{-2}d^{-1}$ and mainly mediated by the bacterial community (DOU/TOU >80 %, Table 2). The new primary production, the part of the total production which can fuel the benthos, in the West Spitsbergen area is in the order of 55 g C $m^{-2}yr^{-1}$ (Sakshaug, 2004, and references therein). This is equal to 38 mmol C $m^{-2}d^{-1}$, assuming a production period of 120 days as suggested by Gradinger (2009). This indicates that approximately 2.6 % of the new primary production in the WS area is remineralised by the benthic activity. However, Lalande et al. (2016) reported from particle trap measurements deployed at HG IV that only 2.7 g C $m^{-2}yr^{-1}$ (= 1.9 mmol C $m^{-2}d^{-1}$ under the same assumption of 120 days of production) and therefore only 5 % of the primary production reaches the seafloor. Taking these export fluxes into account indicates that half of the organic material, that reaches the seafloor, is remineralised by the benthos in the West Spitzbergen area. To our knowledge, there is no data on primary production for the eastern Fram Strait available. However, the EGC is fed by the Transpolar current. Therefore, we assume the same primary production conditions for the EG area as for the central Arctic Ocean. Sakshaug (2004, and references therein) reported a new primary production of <1 g C $m^{-2}yr^{-1}$ (= 0.7 mmol C $m^{-2}d^{-1}$ under the same assumption of 120 days of production) in the central Arctic Ocean. This would indicate that the benthos in the EG area is not only fed by ice- and under-ice algae production because our oxygen consumption values are higher than the new primary production. Annual POC flux values of 1–2.7 g C $m^{-2}yr^{-1}$ (= 0.7–1.9 mmol C $m^{-2}d^{-1}$, under the same assumption of 120 days of production) for the permanently ice-covered northwest water polynya at the Greenland shelf at 80 °N (Bauerfeind et al., 1997) and 1.6 g C $m^{-2}yr^{-1}$ (= 1.1 mmol C $m^{-2}d^{-1}$, under the same assumption of 120 days of production) at the Greenland Shelf at 74 °N ((Bauerfeind et al., 2005) support these findings. Current calculations of the new primary production in the central Arctic Ocean during the sea-ice minimum in 2012 by Fernández-Méndez et al. (2015), who estimated the carbon uptake since the winter water formation from nutrient, salinity

and temperature profiles, found 9.4 g C $m^{-2}yr^{-1}$ (= 6.5 mmol C $m^{-2}d^{-1}$, assuming 120 days of production). This is roughly 10 times higher than the estimations done by Sakshaug (2004, and references therein). Transferring this value to the Fram Strait, >15 % of the surface primary production would be remineralised in the EG area, which is comparable to the Arctic shallow shelves (Grebmeier et al., 1988; Renaud et al., 2007).

However, these numbers have to be interpreted with caution, as a more reliable calculation of the primary production across the entire Fram Strait still remains difficult. Satellite-based chlorophyll measurements are only available in ice-free areas when there are no clouds and no fog (Cherkasheva et al., 2014). Additionally, satellites only measure chlorophyll a in the upper water column. Therefore, to calculate the primary production, additional information about the mixed water depth, photosynthetically active radiation, water temperature, salinity, nutrient availability, the chlorophyll a to carbon ratio, growth rates of the different occurring algae (Sakshaug, 2004) and further parameters needed to be measured during the bloom period, which can be exclusively obtained by ship-based expeditions. Furthermore, the measurements of the benthic oxygen flux, crucial to evaluate the pelagic-benthic-coupling, remain only snapshots of remineralisation. The question, if the Arctic deep-sea benthic oxygen fluxes follow seasonal changes, has only been sparsely evaluated (Bourgeois et al., 2017). A full annual cycle of benthic remineralisation is still missing and as such, a more reliable discussion of the pelagic-benthic-coupling and the carbon cycle remains difficult.

4.3 A future deep-sea benthic Arctic Ocean scenario

Atmospheric and ocean temperatures are increasing globally (IPCC, 2013) and this warming trend amplifies in polar areas (Manabe and Stouffer, 1980; Hassol, 2004). Generally, the warming trend causes a sea-ice thinning (Kwok and Rothrock, 2009), a diminishing sea-ice cover (Comiso et al., 2008), and a decrease of perennial sea-ice (Comiso, 2002). Furthermore, as the annual and the summer sea-ice extent decreases (IPCC 2013), the sea-ice edge is moving northwards. If these trends continue, a sea-ice free Arctic Ocean is predicted for the second half of the century by the Intergovernmental Panel on Climate Change (IPCC 2013), while others (Arzel et al., 2006; Wang and Overland, 2012) predicted it to happen even earlier. Due to its stable sea-ice cover conditions, we can use the Fram Strait to discuss potential consequences for a future deep-sea benthic Arctic Ocean. We compare different stations representing different states of the development from the former towards a predicted future Arctic Ocean. Within our comparison and owing to its specific regional characteristic sea-ice cover, the EG bathymetric transect represents the former Arctic Ocean, while the predicted, future Arctic Ocean is represented by the HG bathymetric transect. Furthermore, the station EG V represents a first transition step and station N5 a second transition step from former to the future Arctic Ocean.

Our results indicate that a development from a permanently sea-ice covered to a seasonally sea-ice covered Arctic Ocean will change the bentho–pelagic relationship from a surface sea-ice dependent towards a water depth dependent environment (Fig. 4). This may go along with a predicted compositional shift in the spring phytoplankton bloom from diatom dominated to coccolithophorid (Bauerfeind et al., 2009) or *Phaeocystis* sp. and nanoflagellates dominated bloom (Soltwedel et al., 2015). An altered algal composition will affect zooplankton communities (Caron and Hutchins, 2013) and

partly organic particle fluxes (Wohlers et al., 2009). An additional predicted effect is an increasing annual matter flux towards the seafloor (Wassmann, 2011; Boetius et al., 2013, this study), while the labile detritus flux is predicted to decrease (Hop et al., 2006; van Oevelen et al., 2011). Therefore, the change in sea-ice cover in the Arctic Ocean may alter the quality and quantity of the organic matter flux to the seafloor, where it maybe affects benthic deep-sea communities (Kortsch et al., 2012; Jones et al., 2014). However, the comparable DOU of the EG and HG site at water depth >1500 m (Fig. 4) indicates that the remineralisation activity of the deep-sea benthos will possibly remain stable in the Arctic Ocean.

Our scenario is only suitable if primary production in the Arctic Ocean would increase as the HG transect and especially N5, EG V and HG IV are located in the highly productive Marginal Ice Zone (Soltwedel et al. (2015). However, the development of future Arctic Ocean primary production patterns and changes is still under debate (Wassmann, 2011, Arrigo et al., 2012; Nicolaus et al., 2012, Boetius et al., 2013). Additionally, the sea ice in the Fram Strait is already thinning (Krumpen et al., 2015). This may be led to more light in the upper water column and an already higher primary production in the EG area, which consequently may have resulted in a higher food supply to the deep-sea benthos in this area and thereby biases our former-Arctic-Ocean perspective. However, fast sinking algae patches as reported by Boetius et al (2013) in the central Arctic, indicative of a higher primary production by ice- and under ice-algae due to changing sea ice conditions, were not observed during a video transect at EG IV in 2014 (pers. Comm. J. Taylor). A further limitation of our scenario might be, that in contrast to the HG stations, there are no long-term data available about the benthic environment at the EG stations. Thus, an assessment of ongoing changes in the EG area, similar to the HG stations (Soltwedel et al., 2015), and getting insight into the natural variability of benthic changes remains difficult at the moment. Nevertheless, the stable sea-ice conditions across the eastern Fram Strait within the last 14 years (Fig. 2) indicates that at least the production period and therefore, the low amount of food supply at the EG stations was also stable within the last 14 years. Besides the limitations of our scenario, the lack of consistent time series data from the entire Arctic Ocean (Wassmann et al., 2011) to create reliable models for future predictions, observations are currently still the best and only method to create scenarios of future developments. Thus, our comparative study provides new insights into the relationship between sea–ice cover at the surface and benthic oxygen fluxes in the Fram Strait via surface primary production, benthic food supply, benthic community and their functions. We hypothesize that if surface primary and secondary production will increase due to the retreating sea–ice cover, the deep-sea benthos of the Arctic Ocean may shift from a sea-ice dependent towards a water depth dependent environment. There might be a slightly increased food supply and an altered macrofauna community, but remineralisation at water depths greater than 1500 m seems to be hardly affected by these changes because it is in any case food limited.

Biogeosciences Discuss., https://doi.org/10.5194/bg-2017-537
Manuscript under review for journal Biogeosciences
Discussion started: 3 January 2018

Figures

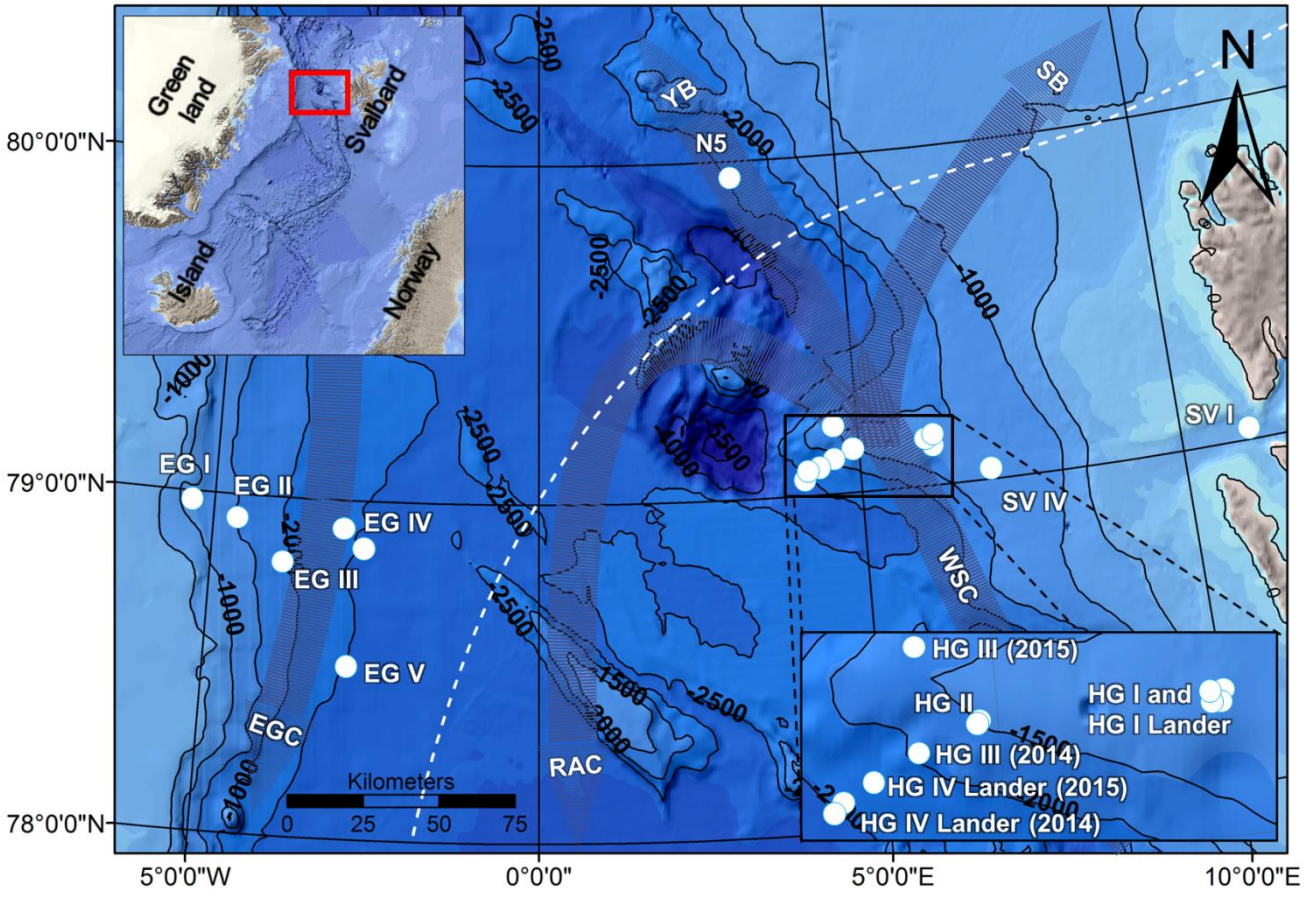

Figure 1. Location of the sampled stations in the Arctic Fram Strait. General summer sea-ice extent: white dashed line. General current system: grey arrows. EGC = East Greenland Current, WSC = West Spitsbergen Current, SB = Svalbard branch, YB = Yermak branch, RAC = Recirculating Atlantic current. More station-specific details are given in Table 1.

Biogeosciences Discuss., https://doi.org/10.5194/bg-2017-537
Manuscript under review for journal Biogeosciences
Discussion started: 3 January 2018

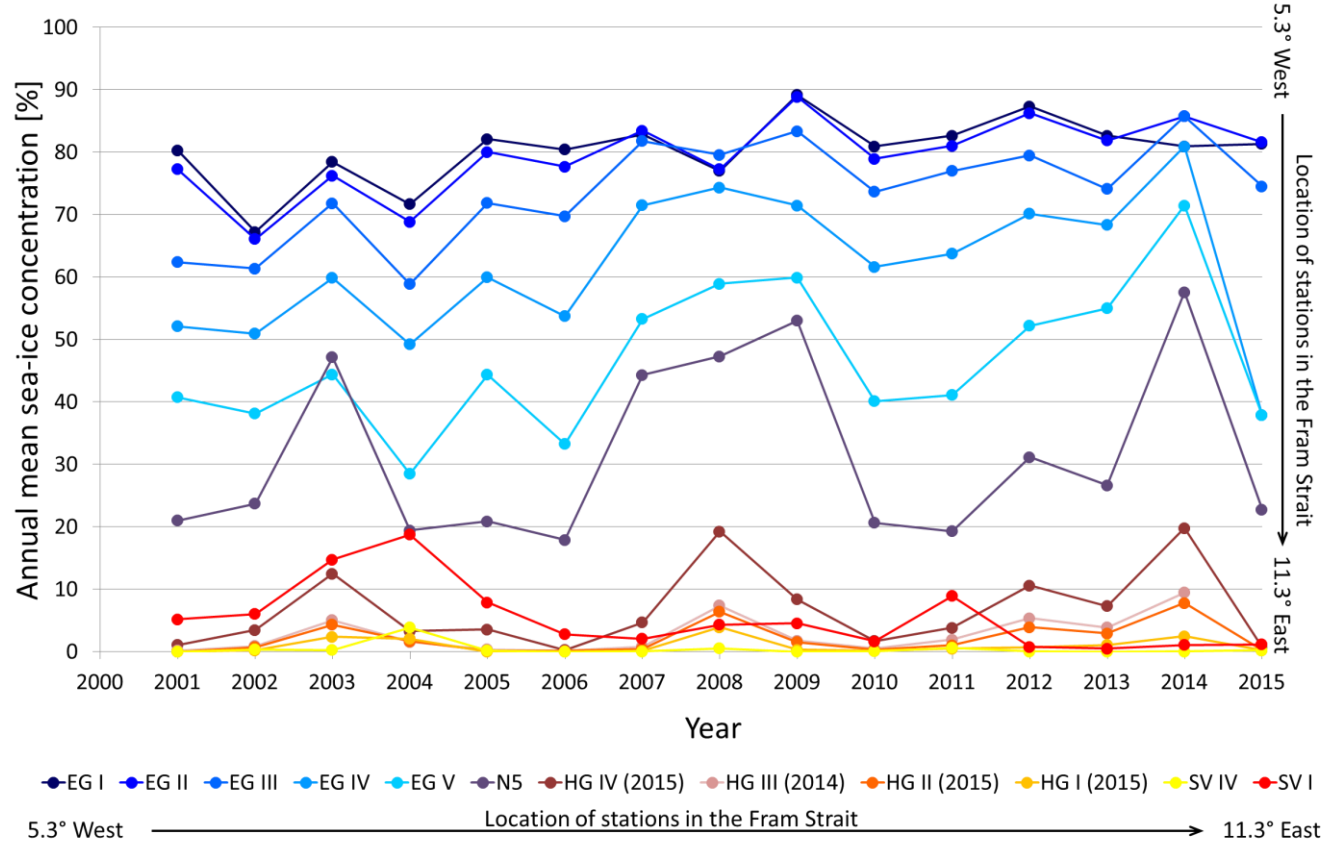

Figure 2. Annual mean sea-ice concentrations from 2001 to 2015 of a subset of the sampled stations. The sampling year at the HG stations is given, as HG stations where sampled in 2014 and 2015 and therefore, the given sampling year refers to the exact position from which the sea ice data were obtained.

Biogeosciences Discuss., https://doi.org/10.5194/bg-2017-537
Manuscript under review for journal Biogeosciences
Discussion started: 3 January 2018

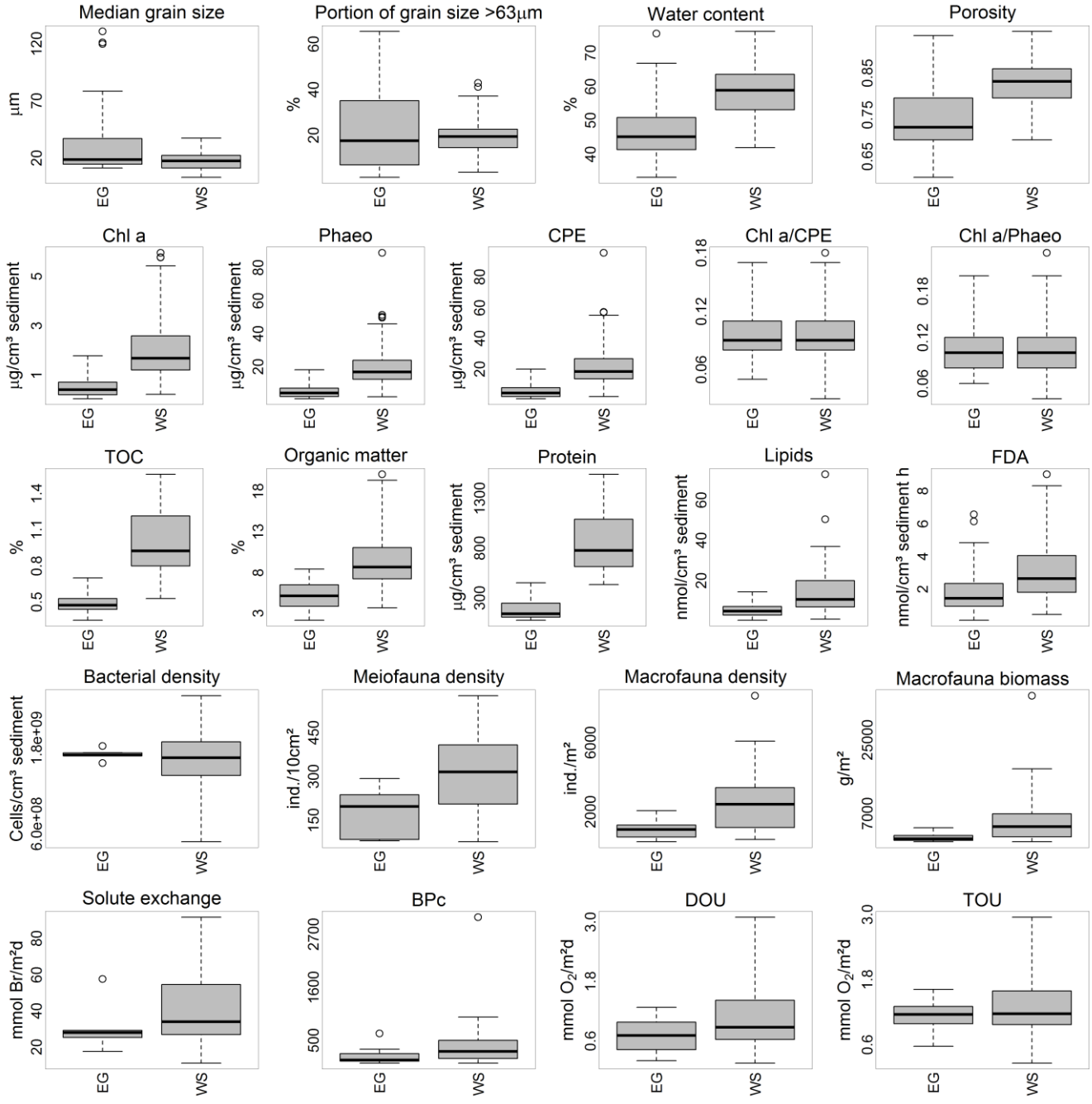

Figure 3. Boxplots of sediment properties, biogenic compound values, benthic community data, oxygen fluxes, from oxygen fluxes conversed carbon fluxes of the EG and WS area. For comparability, the WS site does not contain values from SV I station.

Biogeosciences Discuss., https://doi.org/10.5194/bg-2017-537
Manuscript under review for journal Biogeosciences
Discussion started: 3 January 2018

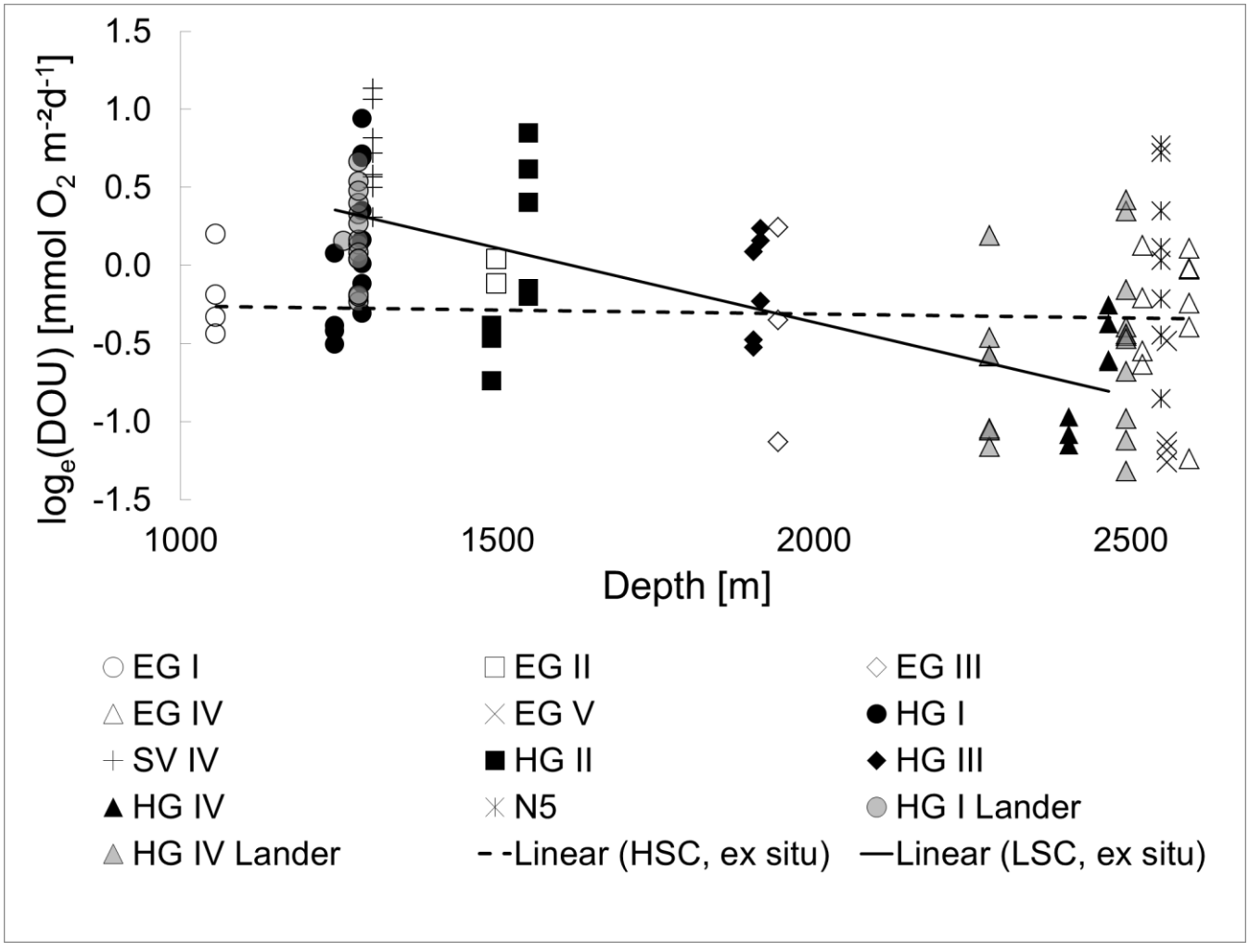

Figure 4. Log-transformed DOU data as a function of water depth at each station and linear regressions in the HSC and LSC categories (from ex situ values). The full line indicates a significant decrease of DOU with water depth in the LSC area, while the dashed line indicates that the slope does not differ significantly from zero.

Biogeosciences Discuss., https://doi.org/10.5194/bg-2017-537
Manuscript under review for journal Biogeosciences
Discussion started: 3 January 2018

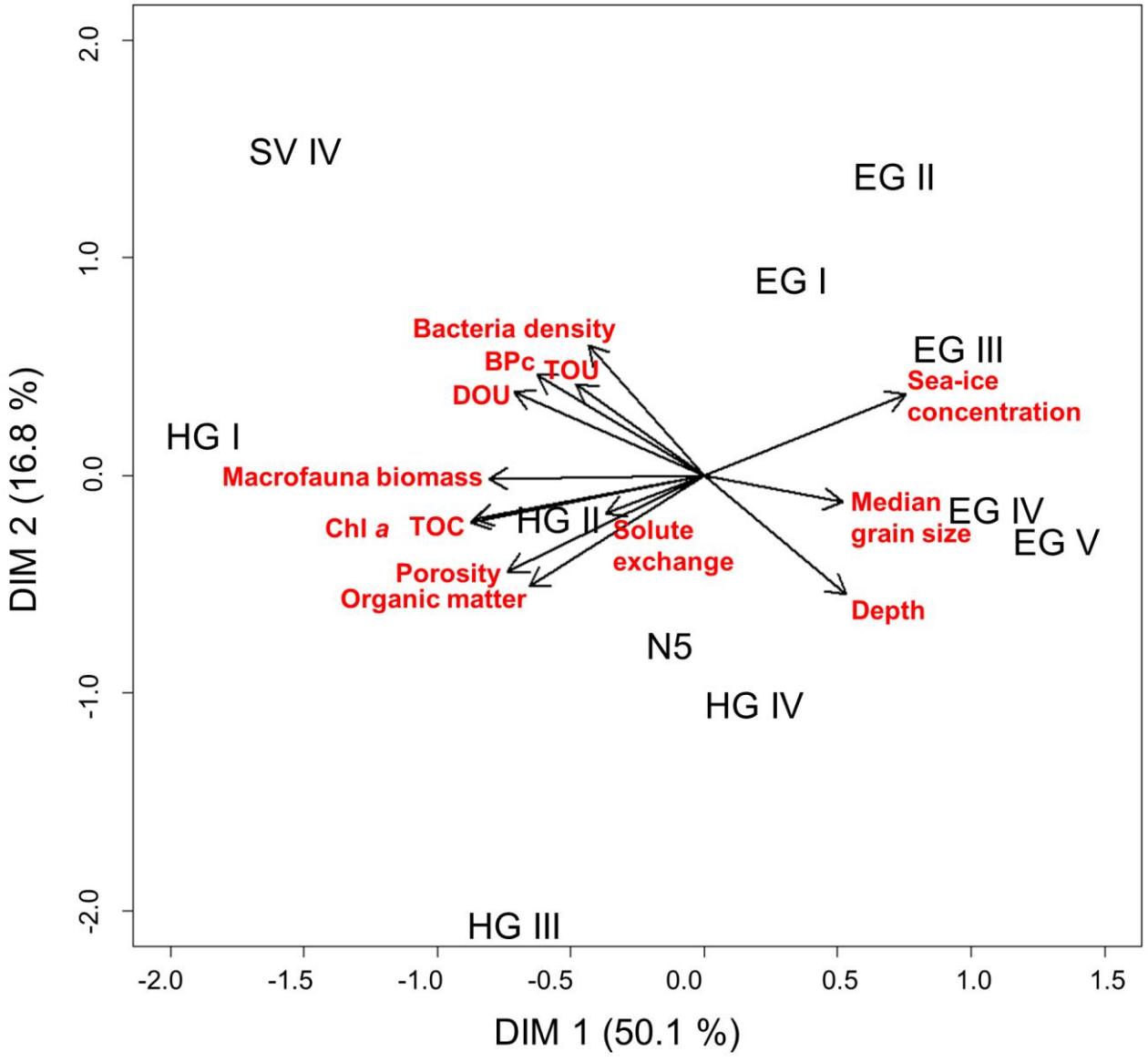

Figure 5. Visualisation of PCA results on standardised ex situ mean values of abiotic parameters (water depth, sea-ice concentration, median grain size, porosity), biogenic compound parameters (Chl *a*, TOC, organic matter), benthic community parameters (bacterial density, macrofauna biomass), macrofauna-mediated environmental functions (Solute exchange, BPc), and oxygen fluxes (DOU, TOU). All other parameters were excluded from the PCA as they correlated strongly with one of the mentioned parameters (correlation >0.74, Pearson correlation, Supplement Table S2). For comparability, Station SV I was excluded from the PCA. Therefore, the figure reflects dependencies of different parameters in the Fram Strait for water depths between 1000–2500 m.

Biogeosciences Discuss., https://doi.org/10.5194/bg-2017-537
Manuscript under review for journal Biogeosciences
Discussion started: 3 January 2018

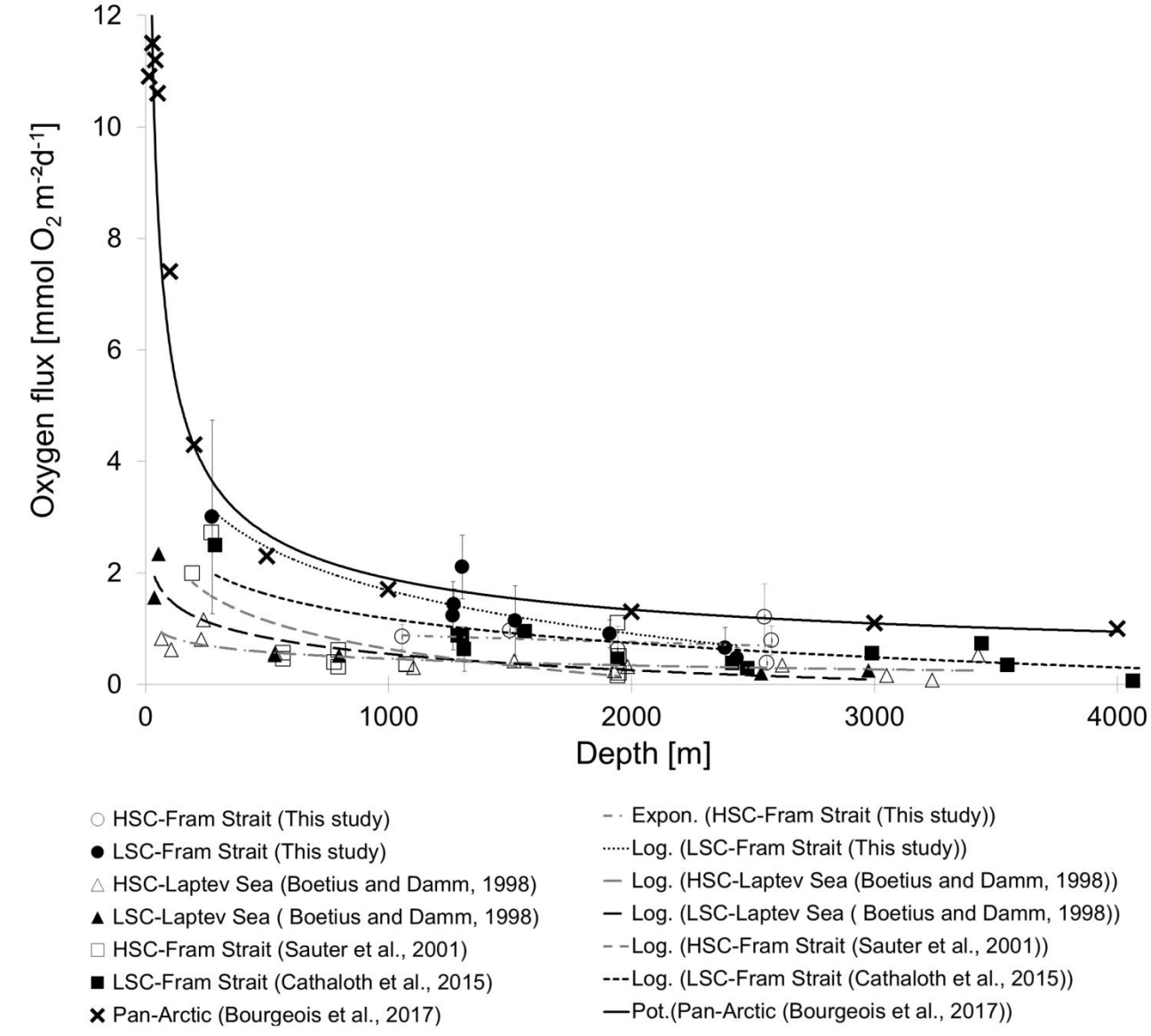

Figure 6. Sediment oxygen uptakes in different water depths (15 m – 4000m) for HSC and LSC sea-ice categories from this study and from literature data for the Laptev Sea, Fram Strait, and Pan-Artic region and related regressions. HSC regression from this study: $y=-0.124\ln(x)+1.7388$ ($R^2=0.0255$); LSC regression from this study: $y=-1.119\ln(x)+9.4144$ ($R^2=0.8695$); HSC regression from Sauter et al (2001): $y=-0.727\ln(x)+5.6587$ ($R^2=0.5026$); LSC regression from Cathalot et al. (2015): $y=-0.63\ln(x)+5.534$ ($R^2=0.7013$); HSC regression from Boetius and Damm (1998): $y=-0.172\ln(x)+1.6496$ ($R^2=0.6074$); LSC regression from Boetius and Damm (1998): $y=-0.421\ln(x)+3.4515$ ($R^2=0.8428$); Pan-Arctic regression from Bourgeois et al (2017): $y=7.1338e^{-6E-04x}$ ($R^2=0.7288$). Regression types were chosen based on best fit (R^2). The model of Bourgeois et al (2017) include DOU and TOU values, while all other references refer only to DOU values.

Data availability

Data are available via the PANGAEA data archive. https://www.pangaea.de/

5

Authors contribution

RH, UB, and FW designed this study; RH and UB were responsible for the measurements and calculations of the oxygen fluxes. Additionally, UB was responsible for the measurement of the grain size parameters and bromide concentrations, and pre-processing and identification of the meio- and macrofauna densities and macrofauna biomasses. CH was responsible for the measurements of the water content and the biogenic compounds. RH was responsible for the calculation of the porosity, the solute exchange, and the BPc and performed all statistical analyses within "R". CH was responsible for the statistical analyses in PRIMER. RH prepared the manuscript with contributions from all co-authors.

Competing interests

The authors declare that they have no conflict of interest.

Acknowledgement

We thank the officers and crew members of RV *Polarstern* for their help during our expeditions to the Fram Strait. Furthermore, we like to thank Volker Asendorf and Axel Nordhausen for preparing the Lander and executing the deployment and recovery during the expeditions, Cäcilia Wiegand and Ines Schröder for the production of the Clark-typ oxygen sensors, Bart Beuselinck for granulometric analyses, Anja Pappert, Svenja Schütte and Meike Spill for biogenic compound and bacterial density analyses, Naomi De Roeck, Thomas Luypaert, Emiel Platjouw, Ellen Pape and Katja Guilini for processing of macro- and meiofauna samples, Thomas Krumpen for providing the additional sea-ice concentrations at station EG V and Pier Buttigieg and Christiane Hassenrück for support regarding statistical analyses in R. This research was funded by the European Union FP7 Project SenseOCEAN Marine Sensors for the 21st century (Grant Agreement Number 614141), by the Flemish Research Fund, by institutional funds of the Alfred -Wegener- Institut Helmholtz-Zentrum für Polar-und Meeresforschung, and by the infrastructure framework of the FRAM project (Frontiers in Arctic Marine Monitoring).

References

Anderson, M. J.: PERMANOVA: Permutational multivariate analysis of variance, Auckland: Department of Statistics, 2005.

Anderson, M. J., Gorley, R. N., Clarke, K. R.: PERMANOVA+ for PRIMER: guide to software and statistical methods, PRIMER-E, Plymouth, 2007.

Ambrose, W. G. and Renaud, P. E.: Benthic response to water column productivity patterns: Evidence for benthic-pelagic coupling in the Northeast Water Polynya, J. Geophys. Res., 100, 4411, doi:10.1029/94JC01982, 1995.

Arrigo, K. R., van Dijken, G., and Pabi, S.: Impact of a shrinking Arctic ice cover on marine primary production, Geophys. Res. Lett., 35, doi:10.1029/2008GL035028, 2008.

Arrigo, K. R., Perovich, D. K., Pickart, R. S., Brown, Z. W., van Dijken, G. L., Lowry, K. E., Mills, M. M., Palmer, M. A., Balch, W. M., Bahr, F., Bates, N. R., Benitez-Nelson, C., Bowler, B., Brownlee, E., Ehn, J. K., Frey, K. E., Garley, R., Laney, S. R., Lubelczyk, L., Mathis, J., Matsuoka, A., Mitchell, B. G., Moore, G. W. K., Ortega-Retuerta, E., Pal, S., Polashenski, C. M., Reynolds, R. A., Schieber, B., Sosik, H. M., Stephens, M., and Swift, J. H.: Massive Phytoplankton Blooms Under Arctic Sea Ice, Science, 336, 1408, doi:10.1126/science.1215065, 2012.

Arzel, O., Fichefet, T., and Goosse, H.: Sea ice evolution over the 20th and 21st centuries as simulated by current AOGCMs, Ocean Modelling, 12, 401–415, doi:10.1016/j.ocemod.2005.08.002, 2006.

Bauerfeind, E., Garrity, C., Krumbholz, M., Ramseier, R. O., and Voβ, M.: Seasonal variability of sediment trap collections in the Northeast Water Polynya. Part 2. Biochemical and microscopic composition of sedimenting matter, Journal of Marine Systems, 10, 371–389, doi:10.1016/S0924-7963(96)00069-3, 1997.

Bauerfeind, E., Leipe, T., and Ramseier, R. O.: Sedimentation at the permanently ice-covered Greenland continental shelf (74°57.7′N/12°58.7′W): significance of biogenic and lithogenic particles in particulate matter flux, Journal of Marine Systems, 56, 151–166, doi:10.1016/j.jmarsys.2004.09.007, 2005.

Bauerfeind, E., Nöthig, E.-M., Beszczynska, A., Fahl, K., Kaleschke, L., Kreker, K., Klages, M., Soltwedel, T., Lorenzen, C., and Wegner, J.: Particle sedimentation patterns in the eastern Fram Strait during 2000–2005: Results from the Arctic long-term observatory HAUSGARTEN, Deep Sea Research Part I: Oceanographic Research Papers, 56, 1471–1487, doi:10.1016/j.dsr.2009.04.011, 2009.

Belcher, A., Iversen, M., Manno, C., Henson, S. A., Tarling, G. A., and Sanders, R.: The role of particle associated microbes in remineralization of fecal pellets in the upper mesopelagic of the Scotia Sea, Antarctica, Limnol. Oceanogr., 61, 1049–1064, doi:10.1002/lno.10269, 2016.

Boetius, A. and Damm, E.: Benthic oxygen uptake, hydrolytic potentials and microbial biomass at the Arctic continental slope, Deep Sea Research Part I: Oceanographic Research Papers, 45, 239–275, doi:10.1016/S0967-0637(97)00052-6, 1998.

Boetius, A. and Lochte, K.: Regulation of microbial enzymatic degradation of organic matter in deep-sea sediments, Marine Ecology Progress Series, 299–307, 1994.

Boudreau, B. P.: Diagenetic models and their implementations: Modelling transport and reactions in aquatic sediments with 75 Fig.s and 19 tables, Springer, Berlin [etc.], XVI, 414 str., 1997.

Bourgeois, S., Archambault, P., and Witte, U.: Organic matter remineralization in marine sediments: A Pan-Arctic synthesis, Global Biogeochem. Cycles, 31, 190–213, doi:10.1002/2016GB005378, 2017.

Braeckman, U., Provoost, P., Gribsholt, B., Van Gansbeke, D., Middelburg, J. J., Soetaert, K., Vincx, M., and Vanaverbeke, J.: Role of macrofauna functional traits and density in biogeochemical fluxes and bioturbation, Mar Ecol Prog Ser, 399, 173–186, doi:10.3354/meps08336, 2010.

Burdige, D. J.: Geochemistry of Marine Sediments, Princeton University Press, Princeton, NJ, xviii, 609, 2006.

Buttigieg, P. L. and Ramette, A.: A guide to statistical analysis in microbial ecology: a community-focused, living review of multivariate data analyses, FEMS Microbiol Ecol, 90, 543–550, doi:10.1111/1574-6941.12437, 2014.

Cathalot, C., Rabouille, C., Sauter, E., Schewe, I., Soltwedel, T., and Vopel, K. C.: Benthic Oxygen Uptake in the Arctic Ocean Margins - A Case Study at the Deep-Sea Observatory HAUSGARTEN (Fram Strait), PLoS ONE, 10, e0138339, doi:10.1371/journal.pone.0138339, 2015.

Cherkasheva, A., Bracher, A., Melsheimer, C., Köberle, C., Gerdes, R., Nöthig, E.-M., Bauerfeind, E., and Boetius, A.: Influence of the physical environment on polar phytoplankton blooms: A case study in the Fram Strait, Journal of Marine Systems, 132, 196–207, doi:10.1016/j.jmarsys.2013.11.008, 2014.

Clarke, K. R. and Gorley, R. N.: Primer v6: User Manual/Tutorial, PRIMER-E, Plymouth, 2006.

Clarke, K. R. and Warwick, R. M.: Similarity-based testing for community pattern: the two-way layout with no replication, Mar. Biol., 118, 167–176, doi:10.1007/BF00699231, 1994.

Comiso, J. C.: A rapidly declining perennial sea ice cover in the Arctic, Geophys. Res. Lett., 29, 17-1, doi:10.1029/2002GL015650, 2002.

Comiso, J. C., Parkinson, C. L., Gersten, R., and Stock, L.: Accelerated decline in the Arctic sea ice cover, Geophys. Res. Lett., 35, doi:10.1029/2007GL031972, 2008.

Donis, D., McGinnis, D. F., Holtappels, M., Felden, J., and Wenzhoefer, F.: Assessing benthic oxygen fluxes in oligotrophic deep sea sediments (HAUSGARTEN observatory), Deep Sea Research Part I: Oceanographic Research Papers, 111, 1–10, doi:10.1016/j.dsr.2015.11.007, 2016.

Ezraty, R., Girard-Ardhuin, F., Piollé, J.-F., Kaleschke, L., and Heygster, G.: Arctic and Antarctic Sea Ice concentration and Arctic Sea Ice drift estimated from Special Sensor Microwave Data: User's Manual, Version 2.1, Département d'Océanographie Physique et Spatiale, IFREMER (Brest, France) and Institute of Environmental Physics, University of Bremen, 2007.

Fernández-Méndez, M., Katlein, C., Rabe, B., Nicolaus, M., Peeken, I., Bakker, K., Flores, H., and Boetius, A.: Photosynthetic production in the central Arctic Ocean during the record sea-ice minimum in 2012, Biogeosciences, 12, 3525–3549, doi:10.5194/bg-12-3525-2015, 2015.

Findlay, R. H., King, G. M., and Watling, L.: Efficacy of Phospholipid Analysis in Determining Microbial Biomass in Sediments, Applied and Environmental Microbiology, 55, 2888–2893, 1989.

Flach, E., Muthumbi, A., and Heip, C.: Meiofauna and macrofauna community structure in relation to sediment composition at the Iberian margin compared to the Goban Spur (NE Atlantic), Progress in Oceanography, 52, 433–457, doi:10.1016/S0079-6611(02)00018-6, 2002.

Forest, A., Wassmann, P., Slagstad, D., Bauerfeind, E., Nöthig, E.-M., and Klages, M.: Relationships between primary production and vertical particle export at the Atlantic-Arctic boundary (Fram Strait, HAUSGARTEN), Polar Biol, 33, 1733–1746, doi:10.1007/s00300-010-0855-3, 2010.

Glud, R. N.: Oxygen dynamics of marine sediments, Marine Biology Research, 4, 243–289, doi:10.1080/17451000801888726, 2008.

Glud, R. N., Gundersen, J. K., Jørgensen, B. B., Revsbech, N. P., and Schulz, H. D.: Diffusive and total oxygen uptake of deep-sea sediments in the eastern South Atlantic Ocean:in situ and laboratory measurements, Deep Sea Research Part I: Oceanographic Research Papers, 41, 1767–1788, doi:10.1016/0967-0637(94)90072-8, 1994.

Gradinger, R.: Sea-ice algae: Major contributors to primary production and algal biomass in the Chukchi and Beaufort Seas during May/June 2002, Deep Sea Research Part II: Topical Studies in Oceanography, 56, 1201–1212, doi:10.1016/j.dsr2.2008.10.016, 2009.

Graf, G., Gerlach, S., Linke, P., Queisser, W., Ritzrau, W., Scheltz, A., Thomsen, L., and Witte, U.: Benthic-pelagic coupling in the Greenland-Norwegian Sea and its effect on the geological record, Geol Rundsch, 84, doi:10.1007/BF00192241, 1995.

Graeve, M. and Ludwichowski, K.-U.: Inorganic nutrients measured on water bottle samples during POLARSTERN cruise PS85 (ARK-XXVIII/2), PANGAEA, 2017, doi.org/10.1594/PANGAEA.882217.

Grebmeier, J. M. and Barry, J. P.: Chapter 11 Benthic Processes in Polynyas, in: Polynyas: Windows to the World, Elsevier Oceanography Series, Elsevier, 363–390, 2007.

Grebmeier, J. M., McRoy, P. C., and Feder, H. M.: Pelagic-benthic coupling on the shelf of the northern Bering and Chukchi Seas. I. Food supply source and benthic biomass, Marine Ecology Progress Series, 48, 57–67, 1988.

Greiser, N. and Faubel, A.: Biotic factors, in: Introduction to the study of meiofauna, Higgins, R. P., and Thiel, H. (Eds.), Smithsonian Institution Press, Washington, D.C, 79–114, 1988.

Harada, N.: Review: Potential catastrophic reduction of sea ice in the western Arctic Ocean: Its impact on biogeochemical cycles and marine ecosystems, Global and Planetary Change, 136, 1–17, doi:10.1016/j.gloplacha.2015.11.005, 2016.

Hassol, S.: Impacts of a warming Arctic: Arctic Climate Impact Assessment, Cambridge University Press, Cambridge, U.K, New York, N.Y, 139 pp., 2004.

Heip, C., Vincx, M., and Vranken, G.: The Ecology of marine nematodes, in: Oceanography and Marine Biology: An Annual Review, Barnes, M. (Ed.), Oceanography and Marine Biology - An Annual Review, 23, 399–489, 1985.

Henson, S. A., Beaulieu, C., and Lampitt, R.: Observing climate change trends in ocean biogeochemistry: when and where, Glob Change Biol, 22, 1561–1571, doi:10.1111/gcb.13152, 2016.

Hobbie, J. E., Daley, R. J., and Jasper, S.: Use of nuclepore filters for counting bacteria by fluorescence microscopy, Applied and Environmental Microbiology, 33, 1225–1228, 1977.

IPCC, 2013: Climate Change 2013: The Physical Science Basis. Contribution of Working Group I to the Fifth Assessment Report of the Intergovernmental Panel on Climate Change [Stocker, T.F., D. Qin, G.-K. Plattner, M. Tignor, S.K. Allen, J. Boschung, A. Nauels, Y. Xia, V. Bex and P.M. Midgley (eds.)]. Cambridge University Press, Cambridge, United Kingdom and New York, NY, USA, 1535 pp, doi:10.1017/CBO9781107415324.

Jahnke, R. A. and Jackson, G. A.: The Spatial Distribution of Sea Floor Oxygen Consumption in The Atlantic and Pacific Oceans, in: Deep-Sea Food Chains and the Global Carbon Cycle, Rowe, G. T., and Pariente, V. (Eds.), Springer Netherlands, Dordrecht, 295–307, 1992.

Klages, M., Boetius, A., Christensen, J. P., Deubel, H., Piepenburg, D., Schewe, I., and Soltwedel, T.: The Benthos of Arctic Seas and its Role for the Organic Carbon Cycle at the Seafloor, in: The Organic Carbon Cycle in the Arctic Ocean, Stein, R., and MacDonald, R. W. (Eds.), Springer Berlin Heidelberg, Berlin, Heidelberg, 139–167, 2004.

Köster, M., Jensen, P., and Meyer-Reil, L.-A.: Hydrolytic Activities of Organisms and Biogenic Structures in Deep-Sea Sediments, in: Microbial Enzymes in Aquatic Environments, Chróst, R. J. (Ed.), Springer New York, New York, NY, 298–310, 1991.

Krumpen, T.: Sea Ice and Atmospheric Conditions at HAUSGARTEN between 2000 - 2016 (daily resolution), link to model results, PANGAEA, 2017.

Krumpen, T., Gerdes, R., Haas, C., Hendricks, S., Herber, A., Selyuzhenok, V., Smedsrud, L., and Spreen, G.: Recent summer sea ice thickness surveys in the Fram Strait and associated volume fluxes, The Cryosphere Discuss., 9, 5171–5202, doi:10.5194/tcd-9-5171-2015, 2015.

Kruskal, J. B.: Multidimensional scaling by optimizing goodness of fit to a nonmetric hypothesis, Psychometrika, 29, 1–27, doi:10.1007/BF02289565, 1964.

Kwok, R. and Rothrock, D. A.: Decline in Arctic sea ice thickness from submarine and ICESat records: 1958-2008, Geophys. Res. Lett., 36, n/a, doi:10.1029/2009GL039035, 2009.

Lalande, C., Nöthig, E.-M., Bauerfeind, E., Hardge, K., Beszczynska-Möller, A., and Fahl, K.: Lateral supply and downward export of particulate matter from upper waters to the seafloor in the deep eastern Fram Strait, Deep Sea Research Part I: Oceanographic Research Papers, 114, 78–89, doi:10.1016/j.dsr.2016.04.014, 2016.

Li, Y.-H. and Gregory, S.: Diffusion of ions in sea water and in deep-sea sediments, Geochimica et Cosmochimica Acta, 38, 703–714, doi:10.1016/0016-7037(74)90145-8, 1974.

Manabe, S. and Stouffer, R. J.: Sensitivity of a global climate model to an increase of CO 2 concentration in the atmosphere, J. Geophys. Res., 85, 5529, doi:10.1029/JC085iC10p05529, 1980.

Manley, T. O.: Branching of Atlantic Water within the Greenland-Spitsbergen Passage: An estimate of recirculation, J. Geophys. Res., 100, 20627, doi:10.1029/95JC01251, 1995.

Nicolaus, M., Katlein, C., Maslanik, J., and Hendricks, S.: Changes in Arctic sea ice result in increasing light transmittance and absorption, Geophys. Res. Lett., 39, n/a, doi:10.1029/2012GL053738, 2012.

Piepenburg, D., Ambrose, W. G., Brandt, A., Renaud, P. E., Ahrens, M. J., and Jensen, P.: Benthic community patterns reflect water column processes in the Northeast Water polynya (Greenland), Journal of Marine Systems, 10, 467–482, doi:10.1016/S0924-7963(96)00050-4, 1997.

Queirós, A. M., Birchenough, Silvana N. R., Bremner, J., Godbold, J. A., Parker, R. E., Romero-Ramirez, A., Reiss, H., Solan, M., Somerfield, P. J., van Colen, C., van Hoey, G., and Widdicombe, S.: A bioturbation classification of European marine infaunal invertebrates, Ecol Evol, 3, 3958–3985, doi:10.1002/ece3.769, 2013.

Quéric, N.-V., Soltwedel, T., and Arntz, W. E.: Application of a rapid direct viable count method to deep-sea sediment bacteria, Journal of Microbiological Methods, 57, 351–367, doi:10.1016/j.mimet.2004.02.005, 2004.

Rasmussen, H. and Jørgensen, B. B.: Microelectrode studies of seasonal oxygen uptake in a coastal sediment: role of molecular diffusion, Mar Ecol Prog Ser, 289–303, 1992.

Redfield, A. C.: On the Proportions of Organic Derivatives in Sea Water and Their Relation to the Composition of Plankton, University Press of Liverpool, 1934.

Reimers, C. E.: An in situ microprofiling instrument for measuring interfacial pore water gradients: methods and oxygen profiles from the North Pacific Ocean, Deep Sea Research Part A. Oceanographic Research Papers, 34, 2019–2035, doi:10.1016/0198-0149(87)90096-3, 1987.

Renaud, P. E., Morata, N., Ambrose, W. G., Bowie, J. J., and Chiuchiolo, A.: Carbon cycling by seafloor communities on the eastern Beaufort Sea shelf, Journal of Experimental Marine Biology and Ecology, 349, 248–260, doi:10.1016/j.jembe.2007.05.021, 2007.

Renner, A. H., Gerland, S., Haas, C., Spreen, G., Beckers, J. F., Hansen, E., Nicolaus, M., and Goodwin, H.: Evidence of Arctic sea ice thinning from direct observations, Geophys. Res. Lett., 41, 5029–5036, doi:10.1002/2014GL060369, 2014.

Revsbech, N. P.: An oxygen microsensor with a guard cathode, Limnol. Oceangr., 34, 474–478, doi:10.4319/lo.1989.34.2.0474, 1989.

Sakshaug, E.: Primary and Secondary Production in the Arctic Seas, in: The Organic Carbon Cycle in the Arctic Ocean, Stein, R., and MacDonald, R. W. (Eds.), Springer Berlin Heidelberg, Berlin, Heidelberg, 57–81, 2004.

Sauter, E. J., Schlüter, M., and Suess, E.: Organic carbon flux and remineralization in surface sediments from the northern North Atlantic derived from pore-water oxygen microprofiles, Deep Sea Research Part I: Oceanographic Research Papers, 48, 529–553, doi:10.1016/S0967-0637(00)00061-3, 2001.

Schauer, U.: Arctic warming through the Fram Strait: Oceanic heat transport from 3 years of measurements, J. Geophys. Res., 109, doi:10.1029/2003JC001823, 2004.

Schewe, I. and Soltwedel, T.: Benthic response to ice-edge-induced particle flux in the Arctic Ocean, Polar Biology, 26, 610–620, doi:10.1007/s00300-003-0526-8, 2003.

Schulz, H. D.: Quantification of Early Diagenesis: Dissolved Constituents in Pore Water and Signals in the Solid Phase, in: Marine Geochemistry, Schulz, H. D., and Zabel, M. (Eds.), Springer Berlin Heidelberg, Berlin, Heidelberg, 73–124, 2006.

Shuman, F. R. and Lorenzen, C. J.: Quantitative degradation of chlorophyll by a marine herbivore, Limnol. Oceangr., 20, 580–586, doi:10.4319/lo.1975.20.4.0580, 1975.

Smith, C. R., De Leo, F. C., Bernardino, A. F., Sweetman, A. K., and Arbizu, P. M.: Abyssal food limitation, ecosystem structure and climate change, Trends in Ecology & Evolution, 23, 518–528, doi:10.1016/j.tree.2008.05.002, 2008.

Smith, K. L.: Benthic community respiration in the N.W. Atlantic Ocean: in situ measurements from 40 to 5200 m, Marine Biology, 47, 337–347, doi:10.1007/BF00388925, 1978.

Smith, K. L., Ruhl, H. A., Kahru, M., Huffard, C. L., and Sherman, A. D.: Deep ocean communities impacted by changing climate over 24 y in the abyssal northeast Pacific Ocean, Proceedings of the National Academy of Sciences, 110, 19838–19841, doi:10.1073/pnas.1315447110, 2013.

Soltwedel, T., Bauerfeind, E., Bergmann, M., Bracher, A., Budaeva, N., Busch, K., Cherkasheva, A., Fahl, K., Grzelak, K., Hasemann, C., Jacob, M., Kraft, A., Lalande, C., Metfies, K., Nöthig, E.-M., Meyer, K., Quéric, N.-V., Schewe, I., Włodarska-Kowalczuk, M., and Klages, M.: Natural variability or anthropogenically-induced variation? Insights from 15 years of multidisciplinary observations at the arctic marine LTER site HAUSGARTEN, Ecological Indicators, doi:10.1016/j.ecolind.2015.10.001, 2015.

Soltwedel, T., Bauerfeind, E., Bergmann, M., Budaeva, N., Hoste, E., Jaeckisch, N., Juterzenka, K. von, Matthiesson, J., Moekievsky, V., Nöthig, E.-M., Quéric, N.-V., Sablotny, B., Sauter, E., Schewe, I., Urban-Malinga, B., Wegner, J., Maria Wlodarska-Kowalczuk, M., and Klages, M.: HAUSGARTEN: Multidisciplinary Investigations at a Deep-Sea, Long-Term Observatory in the Arctic Ocean, oceanog, 18, 46–61, doi:10.5670/oceanog.2005.24, 2005.

Spielhagen, R. F., Müller, J., Wagner, A., Werner, K., Lohmann, G., Prange, M., and Stein, R.: Holocene Environmental Variability in the Arctic Gateway, in: Integrated Analysis of Interglacial Climate Dynamics (INTERDYNAMIC), Schulz, M., and Paul, A. (Eds.), SpringerBriefs in Earth System Sciences, Springer International Publishing, Cham, 37–42, 2015.

Spreen, G., Kaleschke, L., and Heygster, G.: Sea ice remote sensing using AMSR-E 89-GHz channels, J. Geophys. Res., 113, doi:10.1029/2005JC003384, 2008.

Thamdrup, B. and Canfield, D. E.: Benthic Respiration in Aquatic Sediments, in: Methods in Ecosystem Science, Sala, O. E., Jackson, R. B., Mooney, H. A., and Howarth, R. W. (Eds.), Springer New York, New York, NY, 86–103, 2000.

Thiel, H.: Benthos in Upwelling Regions, in: Upwelling Ecosystems, Boje, R., and Tomczak, M. (Eds.), Springer Berlin Heidelberg, Berlin, Heidelberg, 124–138, 1978.

Tremblay, J.-É., Simpson, K., Martin, J., Miller, L., Gratton, Y., Barber, D., and Price, N. M.: Vertical stability and the annual dynamics of nutrients and chlorophyll fluorescence in the coastal, southeast Beaufort Sea, J. Geophys. Res., 113, C07S90, doi:10.1029/2007JC004547, 2008.

Vanreusel, A., Vincx, M., Schram, D., and van Gansbeke, D.: On the Vertical Distribution of the Metazoan Meiofauna in Shelf Break and Upper Slope Habitats of the NE Atlantic, Int. Revue ges. Hydrobiol. Hydrogr., 80, 313–326, doi:10.1002/iroh.19950800218, 1995.

Wang, M. and Overland, J. E.: A sea ice free summer Arctic within 30 years: An update from CMIP5 models, Geophys. Res. Lett., 39, doi:10.1029/2012GL052868, 2012.

Wassmann, P.: Arctic marine ecosystems in an era of rapid climate change, Progress in Oceanography, 90, 1–17, doi:10.1016/j.pocean.2011.02.002, 2011.

Wassmann, P., Duarte, C.M., Agustí, S., Sejr, M.K.:Footprints of climate change in the Arctic marine ecosystem, Global Change Biology, 17, 1235–1249, doi: 10.1111/j.1365-2486.2010.02311.x, 2011

Wenzhöfer, F. and Glud, R. N.: Benthic carbon mineralization in the Atlantic: a synthesis based on in situ data from the last decade, Deep Sea Research Part I: Oceanographic Research Papers, 49, 1255–1279, doi:10.1016/S0967-0637(02)00025-0, 2002.

Wenzhöfer, F., Holby, O., and Kohls, O.: Deep penetrating benthic oxygen profiles measured in situ by oxygen optodes, Deep Sea Research Part I: Oceanographic Research Papers, 48, 1741–1755, doi:10.1016/S0967-0637(00)00108-4, 2001.

Wenzhöfer, F., Oguri, K., Middelboe, M., Turnewitsch, R., Toyofuku, T., Kitazato, H., and Glud, R. N.: Benthic carbon mineralization in hadal trenches: Assessment by in situ O2 microprofile measurements, Deep Sea Research Part I: Oceanographic Research Papers, 116, 276–286, doi:10.1016/j.dsr.2016.08.013, 2016.

Wheatcroft, R. A.: Experimental tests for particle size-dependent bioturbation in the deep ocean, Limnol. Oceanogr., 37, 90–104, doi:10.4319/lo.1992.37.1.0090, 1992.

Winkler, L. W.: Die Bestimmung des im Wasser gelösten Sauerstoffes, Ber. Dtsch. Chem. Ges., 21, 2843–2854, doi:10.1002/cber.188802102122, 1888.

Biogeosciences Discuss., https://doi.org/10.5194/bg-2017-537
Manuscript under review for journal Biogeosciences
Discussion started: 3 January 2018

Tables

Table 1. General station information regarding water depth, sampling date, location and station ID in the data archive Pangaea. Order of stations for each area follows the water depth gradient.

Area	Station name	Water depth (m)	Sampling date	Latitude (ddd.ddd °N)	Longitude (ddd.ddd °E)	Pangaea Station ID
EG	EG I	1056.3	17/06/2014	78.973	-5.290	PS85/0436-1
	EG II	1499.7	18/06/2014	78.933	-4.650	PS85/0441-1
	EG III	1943.8	19/06/2014	78.803	-3.875	PS85/0445-1
	EG IV	2592	31/07/2015	78.862	-2.710	PS93/0058-12
		2518.5		78.914	-2.961	PS93/0058-17
	EG V	2557.7	20/06/2014	78.505	-2.817	PS85/0454-3
WS	SV I	275	06/08/2015	79.028	11.087	PS93/0066-2
	HG I	1244.2	24/06/2014	79.133	6.1065	PS85/0470-3
		1287.7	10/08/2015	79.138	6.0835	PS93/0080-9
	HG I Lander	1257.6	26/06/2014	79.142	6.124	PS85/0476-1
		1282.2	10/08/2015	79.134	6.092	PS93/0080-8
	SV IV	1304	08/08/2015	79.029	6.999	PS93/0074-3
	HG II	1492.3	24/06/2014	79.132	4.906	PS85/0469-2
		1550.2	09/08/2015	79.130	4.902	PS93/0078-2
	HG III	1904.8	24/06/2014	79.106	4.585	PS85/0468-1
		1916	08/08/2015	79.208	4.600	PS93/0077-2
	HG IV	2402.6	22/06/2014	79.065	4.183	PS85/0460-4
		2465.2	27/07/2015	79.065	4.179	PS93/0050-19
	HG IV Lander	2492.6	24/06/2014	79.052	4.138	PS85/0466-1
		2277.5	27/07/2015	79.083	4.337	PS93/0050-18
	N5	2548.2	03/08/2015	79.938	3.193	PS93/0060-10

Biogeosciences Discuss., https://doi.org/10.5194/bg-2017-537
Manuscript under review for journal Biogeosciences
Discussion started: 3 January 2018

Table 2. Mean values ± standard deviation and number of samples in brackets for each measured parameter at each station. Sea-ice concentrations are mean values for the period 01.07.2013–30.06.2014 for stations only sampled in 2014 and 01.08.2014–31.07.2015 for stations only sampled in 2015. For stations sampled in both years, data of both periods were combined. The CPE is the chloroplastic pigment equivalent and the sum of Chl *a* and Phaeo. Chl *a*–CPE ratio indicates the available labile carbon source, while the Chl *a*–Phaeo ratio indicates the relative age of the carbon source. No value could be calculated for solute exchange across the sea-water-interface at EG II. But in order to perform a PCA on the shown data, the solute exchange value at EG II is the mean value of all EG and the N5 stations.

Parameter category	Parameter	Station													
		EG I	EG II	EG III	EG IV	EG V	SV I	HG I	HG I Lander	SV IV	HG II	HG III	HG IV	HG IV Lander	N5
Sea ice	Sea-ice concentration (%)	82 ± 20 (364)	80 ± 21 (364)	75 ± 27 (364)	72 ± 24 (365)	56 ± 34 (364)	1 ± 5 (365	1 ± 7 (729)	1 ± 7 (729)	0.1 ± 2 (365)	4 ± 12 (729)	5 ± 14 (729)	10 ± 21 (729)	9 ± 19 (729)	40 ± 31 (365)
	Days with sea-ice cover (%)	100.00	100.00	100.00	98.00	93.0	6	4.0	4.0	<0.1	13	16	25	24	82
Sediment property	Median grain size (µm)	13.4 ± 1.2 (15)	15.1 ± 1.7 (15)	20.3 ±3.9 (15)	31.6 ± 7.3 (15)	74.2 ± 29.3 (13)	12.3 ± 2.7 (15)	12.7 ± 6.0 (30)	NA	20.4 ± 6.4 (15)	12.7 ± 5.8 (30)	19.3 ± 5.3 (29)	23.8 ± 5.3 (30)	NA	10.4 ± 2.9 (15)
	Porosity	0.76 ± 0.06 (15)	0.73 ± 0.06 (15)	0.71 ± 0.08 (15)	0.73 ± 0.08 (15)	0.68 ± 0.06 (15)	0.75 ± 0.14 (15)	0.88 ± 0.03 (30)	NA	0.8 ± 0.04 (15)	0.85 ± 0.03 (30)	0.80 ± 0.04 (30)	0.77 ± 0.06 (30)	NA	0.84 ± 0.03 (15)
Food availability	CPE (µg ml^{-1} sediment)	4.7 ± 2.6 (15)	4.2 ± 2.7 (15)	3.4 ± 2.5 (15)	7.8 ± 6.1 (15)	7.4 ± 4.2 (15)	80.0 ± 13.1 (15)	34.0 ± 9.7 (30)	18.9 ± 9.9 (10)	26.7 ± 21.3 (14)	20.4 ± 9.6 (29)	22.1 ± 6.7 (30)	13.6 ± 6.7 (30)	10.7 ± 6.2 (15)	16.0 ± 4.2 (13)
	Chl *a*–CPE ratio	0.10 ± 0.02 (15)	0.11 ± 0.02 (15)	0.10 ± 0.02 (15)	0.08 ± 0.01 (14)	0.09 ± 0.02 (15)	0.16 ± 0.02 (15)	0.09 ± 0.02 (30)	0.13 ± 0.03 (10)	0.09 ± 0.01 (15)	0.09 ± 0.02 (30)	0.10 ± 0.02 (30)	0.10 ± 0.02 (30)	0.10 ± 0.02 (15)	0.07 ± 0.02 (15)
	Chl *a*–Phaeo ratio	0.11 ± 0.03 (15)	0.13 ± 0.02 (15)	0.11 ± 0.03 (15)	0.08 ± 0.02 (14)	0.10 ± 0.02 (15)	0.19 ± 0.03 (15)	0.10 ± 0.03 (30)	0.16 ± 0.04 (10)	0.10 ± 0.02 (15)	0.10 ± 0.02 (30)	0.11 ± 0.03 (30)	0.11 ± 0.02 (30)	0.12 ± 0.03 (15)	0.08 ± 0.02 (15)
Other biogenic compounds	TOC (%)	0.55 ± 0.05 (14)	0.44 ± 0.04 (15)	0.45 ± 0.04 (15)	0.51 ± 0.11 (15)	0.53 ± 0.09 (15)	1.58 ± 0.27 (15)	1.37 ± 0.08 (28)	NA	0.98 ± 0.13 (15)	1.05 ± 0.19 (30)	0.92 ± 0.11 (30)	0.69 ± 0.07 (30)	NA	0.88 ± 0.03 (15)
	Organic matter (%)	7.1 ± 1.0 (15)	3.5 ± 0.6 (15)	3.5 ± 0.6 (15)	6.6 ± 0.7 (15)	5.0 ± 0.9 (15)	8.0 ± 2.2 (15)	9.1 ± 2.9 (30)	NA	8.0 ± 1.0 (15)	10.6 ± 1.3 (29)	11.4 ± 3.8 (28)	6.5 ± 0.9 (29)	NA	8.4 ± 0.4 (15)
Benthic community	Bacteria density (Cells 10^9 ml^{-1} sediment)	1.60 (1)	1.57 (1)	1.55 (1)	1.57 ± 0.09 (4)	1.56 (1)	NA	1.79 ± 0.13 (4)	1.14 ± 0.20 (3)	1.83 ± 0.43 (3)	1.81 ± 0.08 (4)	1.29 ± 0.19 (4)	1.49 ± 0.07 (4)	9.28 ± 0.35 (4)	1.54 ± 0.04 (3)
	Meiofauna density (ind. $10cm^{-2}$)	229 (1)	83 (1)	86 (1)	192 ± 79 (4)	245.0	1150 ± 159 (3)	333 ± 134 (3)	357 ± 151 (5)	402 ± 123 (3)	277 ± 75 (4)	273 ± 83 (4)	352 ± 141 (4)	293 ± 202 (6)	268 ± 98 (3)
	Macrofauna biomass (mg m^{-2})	3524 (1)	1971 (1)	1301 (1)	433 ± 287 (3)	450 (1)	45370 ± 25609 (3)	12196 ± 13652 (4)	6929 (1)	8733 ± 1671 (3)	1325 ± 479 (4)	6186 ± 6137 (4)	2784 ± 1578 (4)	836 (1)	8166 ± 7364 (3)
	Macrofauna density (ind. m^{-2})	1414 (1)	991 (1)	284 (1)	1058 ± 722 (3)	1064 (1)	4945 ± 6286 (3)	2860 ± 1206 (4)	942 (1)	4143 ± 2817 (3)	2471 ± 612 (4)	4343 ± 2818 (4)	1148 ± 542 (4)	417 (1)	2023 ± 409 (3)
Community functions	Solute exchange (mmol Br $m^{-2}d^{-1}$)	29.3 (1)	25.3 (1)	57.7 (1)	17.7 (1)	28.1 (1)	38.8 ± 1.8 (3)	51.3 ± 14.1 (4)	NA	39.9 ± 6.3 (3)	38.9 ± 13 (5)	53.2 ± 27.3 (3)	50.8 ± 39.3 (2)	NA	15.0 ± 3.1 (3)

Biogeosciences Discuss., https://doi.org/10.5194/bg-2017-537
Manuscript under review for journal Biogeosciences
Discussion started: 3 January 2018

	BPc	643.7 (1)	317.5 (1)	92.8 (1)	54.8 ± 25.3 (3)	132.4 (1)	1586.1 ± 1041.8 (3)	556.2 ± 266.1 (4)	397.1 (1)	909.2 ± 851.6 (8)	198.7 ± 50.9 (4)	391.2 ± 89.8 (4)	74 ± 40.3 (4)	70.0 (1)	105.5 ± 39.4 (3)
Oxygen flux	DOU (mmol O_2 $m^{-2}d^{-1}$)	0.9 ± 0.2 (4)	1.0 ± 0.1 (2)	0.6 ± 0.4 (4)	0.8 ± 0.3 (4)	0.4 ± 0.1 (10)	3.0 ± 1.7 (6)	1.2 ± 0.6 (12)	1.2 ± 0.3 (15)	2.1 ± 0.6 (8)	1.1 ± 0.6 (8)	0.9 ± 0.3 (7)	0.5 ± 0.2 (8)	0.7 ± 0.4 (18)	1.2 ± 0.6 (8)
	TOU (mmol O_2 $m^{-2}d^{-1}$)	0.9 ± 0.3 (2)	1.6 (1)	1.5 ± 0.1 (2)	1.1 ± 0.1 (2)	1.0 ± 0.2 (4)	5.1 ± 0.2 (3)	1.9 ± 0.6 (5)	1.3 ± 0.2 (4)	1.8 ± 0.2 (3)	1.1 ± 0.2 (5)	1.0 ± 0.2 (5)	1.5 ± 0.5 (5)	0.5 ± 0.2 (5)	1.2 ± 0.3 (3)
	DOU/TOU	1.00	0.63	0.40	0.73	0.40	0.59	0.63	0.92	1.17	1.00	0.90	0.33	1.40	1.00
Carbon flux equivalent	C-DOU (mmol C $m^{-2}d^{-1}$)	0.7 ± 0.2 (4)	0.7 ± 0.2 (2)	0.5 ± 0.3 (4)	0.6 ± 0.2 (10)	0.4 ± 0.1 (4)	2.3 ± 1.3 (6)	1.0 ± 0.5 (12)	0.9 ± 0.3 (15)	1.6 ± 0.4 (8)	1.1 ± 0.7 (8)	0.7 ± 0.2 (7)	0.4 ± 0.1 (8)	0.5 ± 0.3 (18)	0.9 ± 0.5 (8)
	C-TOU (mmol C $m^{-2}d^{-1}$)	0.7 ± 0.3 (2)	1.3 (1)	1.1 ± 0.1 (2)	0.8 ± 0.1 (4)	1.0 ± 0.2 (2)	3.9 ± 0.2 (3)	1.5 ± 0.5 (5)	1.0 ± 0.1 (4)	1.4 ± 0.2 (3)	0.8 ± 0.2 (5)	0.8 ± 0.2 (5)	1.1 ± 0.4 (5)	0.4 ± 0.2 (5)	1.0 ± 0.2 (3)

Biogeosciences Discuss., https://doi.org/10.5194/bg-2017-537
Manuscript under review for journal Biogeosciences
Discussion started: 3 January 2018

Table 3. ANOSIM and SIMPER results of the meio- and macrofauna community within sea-ice categories. The table shows that there are differences in the macrofauna community between the HSC and LSC area, while this is not the case for the meiofauna community. The most contributing taxa regarding the in-group similarity within the sea-ice categories and the dissimilarity between the sea-ice categories are given in Supplement Table 8.

		Meiofauna density		Macrofauna density		Macrofauna biomass	
ANOSIM	Global R	0.143		0.266		0.227	
	p-value	0.036		0.005		0.004	
SIMPER		HSC	LSC	HSC	LSC	HSC	LSC
		In–group similarity	In–group similarity	In–group similarity	In–group similarity	In–group similarity	In–group similarity
		66.0 %	72.5 %	35.4 %	56.1 %	27.4 %	32.0 %
		Dissimilarity between groups		Dissimilarity between groups		Dissimilarity between groups	
		32.1 %		55.9 %		75.3 %	